CFD Study of Welding Fume Behaviour

Gustav Nyrenstedt

Thesis for the degree of Master of Science in Engineering

Division of Fluid Mechanics
Department of Energy Sciences

CFD Study of Welding Fume Behaviour

Gustav Nyrenstedt

June 2016, Lund

This project for the degree of Master of Science in Engineering has been conducted at the Division of Fluid Mechanics, Department of Energy Sciences, Faculty of Engineering, Lund University, and at Enginsoft Nordic AB.

Supervisor at the Division of Fluid Mechanics was Professor Johan Revstedt.

Supervisor at Enginsoft Nordic AB was Project engineer Christoffer Järpner.

Examiner at Lund University was Professor Christoffer Norberg.

The project was carried out in cooperation with Nederman Sverige AB.

Thesis for the Degree of Master of Science in Engineering

ISRN LUTMDN/TMHP-16/5371-SE

ISSN 0282-1990

Fluid Mechanics

Department of Energy Sciences

Faculty of Engineering, Lund University

Box 118, 221 00 Lund

Sweden

www.energy.lth.se

Abstract

It is known from many years of experience and measurements that welding fumes are hazardous to the human body. This is one of the major reasons that Nederman develops suction devices for welding fume. In order to get a better understanding of the fume movement, Nederman is in need of reliable CFD models. The CFD models could potentially show where to place the suction and what parameters to alter in order to achieve less hazardous pollution. Software used for this project are ANSYS CFX, ANSYS DesignModeler (for geometry) and ANSYS Meshing along with modeFRONTIER for evaluations on how different parameters affect the fume flow.

Three different welding methods, namely MIG, TIG and SMA, have been studied. These are three of the most commonly used methods for welding today which is why they are chosen. On each of these methods a three dimensional CFD model has been built and later the fume flow was evaluated. The evaluation showed results such as the creation of vortices around the electrode for the MIG and TIG case. It was also revealed that the fume is in some cases moving along the electrode and handle which can be interesting for suction placement.

In order to detect parameters that are affecting the fume flow to a great extent, a parametric model has been built and a Design of Experiments has been performed. Used here was a two dimensional MIG weld with the shield gas rate, heat release and weld angle as variable parameters. Results were showing that the weld angle and shield gas rate affected the fume movement to a large extent.

On-torch suction is a device for suction placed around the welding handle quite close to the melt. A trade-off between suction of fumes and melt protection from shielding gas is here expected due to the risk of shield gas capture. In order to evaluate this trade-off, an optimization of a two dimensional MIG weld with on-torch suction was performed. Targets were to maximize the amount of fume captured, to maximize the amount of shield gas protecting the melt and to minimize the use of shield gas. Parameters varied to obtain these targets were the shield gas rate and the suction rate. From this optimization it was concluded that there are no design that maximizes both parameters in the range tested. However more parameters such as the height of the suction should also be evaluated before any final conclusions can be made.

As a final conclusion it can be said that three dimensional models of welding are very much possible, although they are time consuming, and these models are very interesting for evaluation of different parameter effects in the future

Keywords: CFD, welding, fume, ANSYS CFX, modeFRONTIER

Table of Contents

Acknowledgements

This master thesis was carried out at the Department of Energy Sciences at the Faculty of Engineering LTH of Lund University and at Enginsoft Nordic AB from January to June 2016. It was originally ordered by Nederman Sverige AB. Mentor at the department of energy has been Professor Johan Revstedt and supervisor at Enginsoft Nordic AB has been Project engineer Christoffer Järpner. Examiner for this thesis was Professor Christoffer Norberg who has done an inspiring work to make my thesis as good as possible. I am very thankful for the help I have received from Johan Revstedt who has always answered my questions. Christian Norman at Nederman AB has also been very helpful and answered my every question very swiftly.

Professors Gerd Johansson, Roland Akselsson, Mats Bohgard and Section Manager Klas Malmqvist of Lund University also have a special place in this thesis since they were the ones making the experiments for my verification case in their youth. Also they have always been available for questions. It is impressive to see that one of you is section manager and three of you have reached the status of professor today.

I would also like to thank the fantastic people working at Enginsoft Nordic AB for their everyday support. Especially Sarah, with whom I have been sharing office during my entire thesis, and Ragnar who has taken time to aid me many times.

Finally, my major thanks is going to my supervisor Christoffer, without whom this thesis would not be possible. I am especially thankful that he has always been available even though he has not always had the time.

Lund, June 2016

Gustav Nyrenstedt

Notations

Abbreviations

CFD – Computational fluid dynamics

DOE – Design of experiment

ISF – Incremental space filler

MIG – Metal inert gas

MOGA – Multi-objective genetic algorithm

SMA – Shielded metal arc

TIG – Tungsten inert gas

ULH – Uniform Latin Hypercube

Nomenclature

E_B – Radiated energy

$L_{f,D}$ – Lipschitz constant

$\dot{Q}$ – Rate of heat

$\dot{W}$ – Rate of work

q_{cd} – Heat conduction

q_{cv} – Heat convection

t_∞ - Free stream temperature

t_w – Wall temperature

u_* – Friction velocity

F – Force

I – Radiation intensity

m - Mass

T – Temperature

t – Time

V – Volume

y+ - Dimensionless distance to the wall

α – Heat transfer coefficient

ε – Emissivity

μ – Dynamic viscosity

ρ – Density

σ – Stefan-Boltzmann's constant

τ – Viscous stress

υ – Kinematic viscosity

λ – Thermal conductivity

1. Introduction

Here the value and aim of this master thesis will be presented along with limits of the project as well as the structure of the report.

1.1. Background

Nederman is a world leading provider and developer of products in the environmental technology sector. One part of this is industrial applications such as suction of welding fumes. Welding fumes are known to contain particles and substances that are very dangerous to the human body. Examples of effects can be cancer, lung damage and premature death.

Special legislations for welding fumes exists today and are of course a great motivation for industries to reduce the pollutant. Because of this, Nederman's products for welding suction are very important and provide a safe and easy way of not exposing welders to the hazards of breathing the smoke.

In order to know where the suction should be placed and what operating suction rate that should be used, it is interesting to know how the fumes are moving when released.

1.2. Purpose and Aim

The project is aiming to solve the problem formulation, stated as: "The task is to create accurate, as well as fast, three dimensional CFD models which captures the behaviour of particles and fumes from different welding processes". This will improve knowledge of a part of welding that is affecting human health negatively. The aim is also to evaluate the correlations between certain parameters and the fume movement in the domain.

1.3. Delimitations

This project has been constrained to three different welding methods, namely the MIG, TIG and SMA, in three dimensions and just the MIG method for optimization and testing of different parameters. It is also assumed that all electricity is direct current and released as heat.

Welding fumes released will be assumed to contain particles small enough to be considered a fluid containing the different materials released. The viscosity of this fluid will be similar to a standard ideal gas. Density and thermal conductivity will however be set as the one of the solid fume materials at start.

Since one of the aims with the project is to create a fast model it was decided that the parametrization and optimization cases are to be modelled in two dimensions. Three dimensional models are quite costly when it comes to computational power, due to the larger domain and more complex flow, which is why two dimensional models suits this project better. It has also been concluded from evaluation that the two dimensional models are sufficient to test most parameters, although not all geometry parameters such as the welding angle.

Specific delimitations will be described separately for each case.

1.4. Thesis Outline

The report begins with a short introduction, in chapter one, that contains the background and purpose of the project. Chapter two follows with a theory section describing the necessary aspects to perform this project. Both physical phenomena and mathematical methods will be discussed.

General methods will be brought up in chapter four with geometry, mesh and setup. Following this will be the case specific chapters five to eight. In these chapters all the cases physical phenomena testing, three dimensional welding, parameter testing and the on-torch optimization are described in detail and results are presented and evaluated.

As final part of the thesis, a discussion and conclusion chapter will be presented.

2. Theory

In this chapter the theory needed and used in this thesis will be briefly described. Extra care will be taken to the parts actually applied in the final setup.

2.1. Welding basics

Welding is a very common method for merging different parts of metal. It can for example be used in industries such as the automotive industry. There are a large number of welding methods but in this report only three will be considered. This is mainly due to the fact that these methods are some of the most commonly used today. With these three approaches, a large percent of all welding is covered.

2.1.1. Shielded Metal Arc Welding (SMA)

This type of welding is also called manual metal arc welding (MMAW) or stick welding in everyday speech. It is one of the most used welding methods in the world much due to its simplicity. In welding, shield gas is used to protect the melt from the surroundings. For example to prevent oxidation when the melt is in contact with the air. Characteristic for the SMA method is the fact that the shield gas comes from the coating of the electrode. This means that no separate device for shielding gas is needed and the equipment is very portable. The electrode is consumed during welding and has to be replaced when used up. There are a large number of different electrode types that are used for different kinds of welding materials (see for example ESAB.se for more information). The welding materials when this method is used include different types of steel, aluminium and copper alloys.

2.1.2. Metal Inert Gas Welding (MIG)

The MIG method is, like stick welding, a very common method for welding. Benefits with this method is that it is quite versatile and also fast. This means that for example automotive industries use this method to a large extent. Materials that are welded with MIG include for instance sheet metals. MIG uses a flow of shield gas that is usually fed from around the handle. There are some different types of shield gas composition containing different amounts of carbon dioxide (CO2) and the noble gas argon (Ar). The electrode in MIG welding is a wire that is continuously fed to replace its continuously consumed part. Wires can consist of many different materials and different wires are used for different types of welding materials.

2.1.3. Tungsten Inert Gas Welding (TIG)

TIG welding is the final method that will be considered in this project. This method is quite similar to the MIG method and uses a shielding gas which is fed continuously. However, the tungsten electrode is not consumed during welding and so does not have to be provided or replaced. If supplementary material is needed an extra filler can be used.

2.1.4. Fume Generation from Welding

It has been known for many years that welding releases fumes that are dangerous to the human body. The generation of these fumes comes from vaporization of the metals. How much fume that is generated and the composition depends on the welding method, materials (especially the consumable), shielding gas/coating and the heat while welding. Examples of dangerous fumes and particles produced are ozone, carbon monoxide and hexavalent chromium. These three substances are known to be potentially very toxic. Hexavalent chromium is a known carcinogen as well as irritating to the skin and breathing system (OSHA, u.d.). Ozone and carbon monoxide affects the respiration system (EPA, u.d.) and carbon monoxide can potentially cause death (OSHA, u.d.). Considerable for the fume is the fact that smaller particles are more dangerous to humans, often due to the fact that they enter deeper into the lungs.

2.1.5. Regulations Regarding Fume Release

In order to reduce the amount of fumes from welding, many different regulation systems have been set up. OSHA 2006 is an example of these. It regulates the amount of particles as well as the welder's

clothing, ventilation, respiratory protection and hazard communication. Notable is that with this standard the maximum limit of hexavalent chromium release was reduced more than ten times in comparison with the previous standard. Standards like this are enhancing the development of cleaning the air from welding fumes as well as aiming for a low release.

2.2. Heat Transfer

Heat is the energy that is transferred between bodies due to the difference in temperature between them. There are three different ways of heat transfer, namely conduction, convection and finally radiation.

2.2.1. Conduction

Conduction is the heat transfer in a material due to the movement of molecules and can occur in all kinds of materials where there are varying temperatures. The definition of heat conduction, q_{cd} $[\frac{W}{m^2}]$, is written as:

$$q_{cd} = -\lambda \frac{\partial t}{\partial n} \quad (1)$$

where $\frac{\partial t}{\partial n}$ is the temperature gradient in the normal direction and λ the thermal conductivity $[\frac{W}{mK}]$.

The thermal conductivity is basically a material's capability of heat transfer.

2.2.2. Convection

Convection is the heat transfer between a fluid and a solid, for example between a water flow in a pipe and the pipe wall.

A way to write the convection, q_{cv}, is with the heat transfer coefficient α $[\frac{W}{m^2K}]$ as follows:

$$q_{cv} = \alpha(t_w - t_\infty) \quad (2)$$

where $t_w - t_\infty$ is the difference between the wall temperature and the surrounding fluid temperature. The heat transfer coefficient is quite complex and depends on a number of factors. Deciding this coefficient is often the largest problem when it comes to calculating convection.

2.2.3. Radiation

The final category of heat transfer is the radiation. This is the heat that a body emits because of its temperature and becomes a significant part of the heat generation when very high temperatures occurs. Some bodies can be described as black bodies which means that they are a perfect emitter and perfect absorber. The radiated energy, E_B, released from black bodies can be described by the Stefan-Boltzmann's law as follows:

$$E_B = \sigma T^4 \quad (3)$$

where T is the temperature [K] and σ the Stefan-Boltzmann constant $[\frac{W}{m^2K^4}]$ which has the value of $5.67 * 10^{-8}$.

Bodies that are not black can be described in terms of how much they coincide with a black body through the emissivity ε. The relation now becomes:

$$E_B = \varepsilon\sigma T^4 \quad (4)$$

Notable for these relations are the fact that the energy is very temperature dependent and with very high temperatures, the radiation will have great significance to the heat transfer.

2.2.3.1. Radiation Models

There are a number of different models that are used to calculate radiation. Here three of the most common ones will be briefly described. Namely the Monte Carlo model, the P1 model and the discrete transfer model.

2.2.3.1.1. Monte Carlo

This method is based on the fact that radiation essentially are photons that are moving and interacting with their surroundings. A photon is tracked and the physical quantities of it are updated every time something happens. Example of what could happen is surface intersection, absorption and scattering. This tracking is ongoing as long as the photon is above a certain weight and the process is done for many photons simultaneously in order to reach satisfying results.

The interactions are a function of photon energy, geometry, density structure and composition of the medium (Astronomy Group, University of St Andrews, u.d.). Absorption means that the photon bounds energy which leads to emitting a new photon. Scattering on the other hand is when the photon change direction and energy level.

Monte Carlo is a very accurate method, however it takes a lot of time to calculate since it needs many photons to get an accurate result which is why it is not chosen for fluid radiation here.

2.2.3.1.2. Discrete Transfer

Unlike the Monte Carlo method, discrete transfer is based on radiation rays. These rays sum up all radiation behaviour and energy. The equation of radiation intensity of a ray is written as follows:

$$\frac{dI}{ds} + aI = \frac{aT^4\sigma}{\pi} \quad (5)$$

where I is the intensity [$\frac{W}{m^2}$], s the distance of the ray [m], a the gas absorption coefficient [m^{-1}], σ Stefan-Boltzmann's constant [$\frac{W}{m^2K^4}$] and T the temperature [K]

Equation (5) is then integrated over a number of rays. If a is constant along the ray it follows from estimation that

$$I(s) = \frac{T^4\sigma}{\pi} * (1 - e^{-as}) + I_0 * e^{-as} \quad (6)$$

where I_0 is the radiant intensity at zero distance.

Finally the summation of the change in intensity over each of the ray's path gives the radiation energy.

One problem with this method is that if the rays are emitted from many different surfaces it takes a lot of computational power to obtain a solution. However it is quite a simple model that can be used for a number of cases. It is also simple to improve the accuracy by just adding more rays (ANSYS Fluent, u.d.)

2.2.3.1.3. P1

This method is also called the differential approximation and has its foundation in adding an extra equation for transport. P1 is generally based on expansion of radiation intensity and is calculated by first setting the radiation flux with the help of the transport equation for the incident radiation. When the radiation flux is decided, it can easily be substituted to radiation energy with the use of its gradient. Since this method is not used in this project it will not be further described here. The reason that it is not used is its problem with localized heat sources (Fluent incorporated, u.d.) which is exactly what is present in this project.

2.3. Computational Fluid Dynamics (CFD)

CFD is a computational method based on the fundamentals of fluid mechanics and heat transfer. It mainly uses a set of governing equations in order to calculate various parameters such as fluid flow and temperature. Some of the most important of these governing equations are the Navier-Stokes which will be presented further in this section.

2.3.1. Governing Equations

The governing equations comes from the conservation laws of physics and are mass conservation, Newton's second law and the first law of thermodynamics.

2.3.1.1. Mass Conservation

The continuity equation or mass conservation states that for a fixed control volume V [m^3], the rate of mass change within must be equivalent to the mass flux crossing the boundary surface S [m^2]. In equation form, this becomes an integral as follows:

$$\frac{d}{dt}\int_V \rho dV = -\int_S \rho V * \bar{\boldsymbol{n}} dS \quad (7)$$

where ρ [kg/m^3] is the density of the fluid and $\bar{\boldsymbol{n}}$ the unit vector normal to the boundary surface.

With the use of Gauss' divergence theorem, Eq. 7 can be written as follows:

$$\int_V \left[\frac{\partial \rho}{\partial t} + \nabla * (\rho V)\right] dV = 0 \quad (8)$$

This equation is general and can be written for any volume V which gives:

$$\frac{\partial \rho}{\partial t} + \nabla * (\rho V) = 0 \quad (9)$$

which is the mass conservation.

2.3.1.2. Newton's Second Law

The momentum equation or Newton's second law states that the sum of forces is equal to the mass multiplied with acceleration. In this case a fluid element with the side lengths $\Delta x, \Delta y$ and Δz is considered. The force F acting on this fluid element is divided into an x-component F_x, a y-component F_y and a z-component F_z.

Using Newton's second law in the x-direction, we get:

$$\sum F_x = ma_x \quad (10)$$

where m is the mass [kg] and a_x the acceleration [m/s] in the x-direction.

Using v_x as notation for the velocity in the x-direction, the acceleration can be written as:

$$a_x = \frac{dv_x}{dt} \quad (11)$$

The mass is equal to the density multiplied with volume as follows:

$$m = \rho * \Delta x \Delta y \Delta z \quad (12)$$

Combining Eq. 11 and 12 gives:

$$ma_x = \rho \frac{Dv_x}{Dt} \Delta x \Delta y \Delta z \quad (13)$$

The force acting on the fluid element in the x-direction can be divided into surface forces and body forces, where the body forces are due to gravity, centrifugalism, Coriolis and electromagnetic forces (J.Tu, 2013). Surface forces are due to normal stress σ_{xx} and tangential stresses τ_{yx} and τ_{zx} acting on

the surfaces. Assuming a Newtonian fluid and isotropic conditions and due to Newton's law of viscosity, these can be written as follows:

$$\sigma_{xx} = -p + \tau_{xx} \tag{14}$$

$$\tau_{xx} = 2\mu \frac{\partial v_x}{\partial x} + \lambda[\frac{\partial v_x}{\partial x} + \frac{\partial v_y}{\partial y} + \frac{\partial v_z}{\partial z}] \tag{15}$$

$$\tau_{yx} = \mu(\frac{\partial v_y}{\partial x} + \frac{\partial v_x}{\partial y}) \tag{16}$$

$$\tau_{zx} = \mu(\frac{\partial v_y}{\partial x} + \frac{\partial v_x}{\partial y}) \tag{17}$$

where P is the pressure [Pa], τ_{xx} is the viscous stress component perpendicular to the control volume, μ the dynamic viscosity relating stress to linear deformation and λ the dynamic viscosity that relates stress to volumetric deformation.

In the y –and z-direction these equations become:

$$\sigma_{yy} = -p + \tau_{yy} \tag{18}$$

$$\tau_{yy} = 2\mu \frac{\partial v_y}{\partial y} + \lambda[\frac{\partial v_x}{\partial x} + \frac{\partial v_y}{\partial y} + \frac{\partial v_z}{\partial z}] \tag{19}$$

$$\tau_{yz} = \mu(\frac{\partial v_z}{\partial y} + \frac{\partial v_y}{\partial z}) \tag{20}$$

$$\sigma_{zz} = -p + \tau_{zz} \tag{21}$$

$$\tau_{zz} = 2\mu \frac{\partial v_z}{\partial z} + \lambda[\frac{\partial v_x}{\partial x} + \frac{\partial v_y}{\partial y} + \frac{\partial v_z}{\partial z}] \tag{22}$$

The total forces can be written as the sum between body forces and surface forces. With the help of Eq. 13 it follows that:

$$\rho \frac{Dv_x}{Dt} = \frac{\partial \sigma_{xx}}{\partial x} + \frac{\partial \tau_{yx}}{\partial y} + \frac{\partial \tau_{zx}}{\partial z} + \sum F_x^{body\ forces} \tag{23}$$

$$\rho \frac{Dv_y}{Dt} = \frac{\partial \sigma_{yy}}{\partial y} + \frac{\partial \tau_{yx}}{\partial x} + \frac{\partial \tau_{yz}}{\partial z} + \sum F_y^{body\ forces} \tag{24}$$

$$\rho \frac{Dv_z}{Dt} = \frac{\partial \sigma_{zz}}{\partial z} + \frac{\partial \tau_{xz}}{\partial x} + \frac{\partial \tau_{yz}}{\partial y} + \sum F_z^{body\ forces} \tag{25}$$

When combining Eq. 14-22 with 23-25 it follows that:

$$\rho \frac{Dv_x}{Dt} = -\frac{\partial p}{\partial x} + \frac{\partial}{\partial x}\left[2\mu \frac{\partial v_x}{\partial x} + \lambda\left(\frac{\partial v_x}{\partial x} + \frac{\partial v_y}{\partial y} + \frac{\partial v_z}{\partial z}\right)\right] + \frac{\partial}{\partial y}\left[\mu\left(\frac{\partial v_x}{\partial y} + \frac{\partial v_y}{\partial x}\right)\right] + \frac{\partial}{\partial z}\left[\mu\left(\frac{\partial v_x}{\partial z} + \frac{\partial v_z}{\partial x}\right)\right] + \sum F_x^{body\ forces} \tag{26}$$

$$\rho \frac{Dv_y}{Dt} = -\frac{\partial p}{\partial y} + \frac{\partial}{\partial y}\left[2\mu \frac{\partial v_y}{\partial y} + \lambda\left(\frac{\partial v_x}{\partial x} + \frac{\partial v_y}{\partial y} + \frac{\partial v_z}{\partial z}\right)\right] + \frac{\partial}{\partial x}\left[\mu\left(\frac{\partial v_x}{\partial y} + \frac{\partial v_y}{\partial x}\right)\right] + \frac{\partial}{\partial z}\left[\mu\left(\frac{\partial v_y}{\partial z} + \frac{\partial v_z}{\partial y}\right)\right] + \sum F_y^{body\ forces} \tag{27}$$

$$\rho \frac{Dv_z}{Dt} = -\frac{\partial p}{\partial z} + \frac{\partial}{\partial z}\left[2\mu \frac{\partial v_z}{\partial z} + \lambda\left(\frac{\partial v_x}{\partial x} + \frac{\partial v_y}{\partial y} + \frac{\partial v_z}{\partial z}\right)\right] + \frac{\partial}{\partial x}\left[\mu\left(\frac{\partial v_x}{\partial z} + \frac{\partial v_z}{\partial x}\right)\right] + \frac{\partial}{\partial y}\left[\mu\left(\frac{\partial v_y}{\partial z} + \frac{\partial v_z}{\partial y}\right)\right] + \sum F_z^{body\ forces} \tag{28}$$

Eq. 26-28 are the momentum equations and can, along with the continuity equations, be rewritten into the Navier-Stokes equations. The assumptions necessary are that the flow is two dimensional and that the body forces can be neglected. Navier-Stokes equations now follows as:

$$\frac{Dv_x}{Dt} = -\frac{1}{\rho}\frac{\partial p}{\partial x} + \frac{\mu}{\rho}\frac{\partial^2 v_x}{\partial x^2} + \frac{\mu}{\rho}\frac{\partial^2 v_x}{\partial y^2} \tag{29}$$

$$\frac{Dv_y}{Dt} = -\frac{1}{\rho}\frac{\partial p}{\partial y} + \frac{\mu}{\rho}\frac{\partial^2 v_y}{\partial x^2} + \frac{\mu}{\rho}\frac{\partial^2 v_y}{\partial y^2} \tag{30}$$

2.3.1.3. First Law of Thermodynamics

This law states that energy cannot be destroyed, only transformed. It follows that the time rate of change of energy ($\frac{DE}{Dt}$) is equal to the sum of rate of heat added and rate of work done as follows:

$$\frac{DE}{Dt} = \sum \dot{Q} + \sum \dot{W} \quad (31)$$

where $\dot{Q}$ is the rate of heat [W] added into the control volume and $\dot{W}$ is the rate of work [W] done by surface forces on the fluid element. For the moving fluid element and if $\frac{DE}{Dt}$ instead is written per unit mass, the time rate of energy change can be written:

$$Time\ rate\ of\ energy\ change = \rho \frac{DE}{Dt} \Delta x \Delta y \Delta z \quad (32)$$

The rate of heat addition in the x-direction can be written as the difference in heat input and heat loss:

$$\sum \dot{Q}_x = [q_x + \frac{\partial q_x}{\partial x} \Delta x] \Delta y \Delta z - q_x \Delta y \Delta z \quad (33)$$

This is similar in the y –and z-directions.

Concerning the rate of work in the x-direction it can be rewritten, using that it is equivalent to the velocity and force, as:

$$\left[v_x \sigma_{xx} + \frac{\partial (v_x \sigma_{xx})}{\partial x} \Delta x\right] \Delta y \Delta z - v_x \sigma_{xx} \Delta y \Delta z \quad (34)$$

for the force in the normal direction, and

$$\left[v_x \tau_{yx} + \frac{\partial (v_x \tau_{yx})}{\partial y} \Delta y\right] \Delta x \Delta z - v_x \tau_{yx} \Delta x \Delta z \quad (35)$$

$$\left[v_x \tau_{zx} + \frac{\partial (v_x \tau_{zx})}{\partial z} \Delta z\right] \Delta x \Delta y - v_x \tau_{zx} \Delta x \Delta y \quad (36)$$

for the forces in the tangential x-direction.

With the use of Eq. 31-36 and dividing with the volume of the fluid element, the equation for the first law of thermodynamics now becomes:

$$\rho \frac{DE}{Dt} = \frac{\partial (v_x \sigma_{xx})}{\partial x} + \frac{\partial (v_y \sigma_{yy})}{\partial y} + \frac{\partial (v_z \sigma_{zz})}{\partial z} + \frac{\partial (v_x \tau_{yx})}{\partial y} + \frac{\partial (v_x \tau_{zx})}{\partial z} + \frac{\partial (v_y \tau_{xy})}{\partial x} + \frac{\partial (v_y \tau_{zy})}{\partial z} + \frac{\partial (v_z \tau_{xz})}{\partial x} + \frac{\partial (v_z \tau_{yz})}{\partial y} - \frac{\partial q_x}{\partial x} - \frac{\partial q_y}{\partial y} - \frac{\partial q_z}{\partial z} \quad (37)$$

With the use of Fourier's law the energy fluxes and with addition of the radiation term S_r, q_i can be rewritten and the first law of thermodynamics is now concluded as:

$$\rho \frac{DE}{Dt} = \frac{\partial}{\partial x}\left[\lambda \frac{\partial T}{\partial x}\right] + \frac{\partial}{\partial y}\left[\lambda \frac{\partial T}{\partial y}\right] + \frac{\partial}{\partial z}\left[\lambda \frac{\partial T}{\partial z}\right] - \frac{\partial (v_x p)}{\partial x} + S_r \quad (38)$$

where T is the temperature [K] and λ the thermal conductivity [W/mK].

2.3.2. Discretization

In order to solve the differential governing equations now described, it is beneficial to make some kind of discretization. In CFD there are two common methods, namely the finite difference method and the finite volume method. A third method is the finite element method but it is not commonly used in CFD despite its ability to handle arbitrary geometries. The biggest con is that it requires much computational power compared to the other two methods and has therefore been set aside in CFD use. Here, only the two most common methods will be presented.

2.3.2.1. Finite Differences

The finite difference method is one of the oldest methods for solving partial differential equations. It is based on using all nodes of the grid to obtain an approximation. The distance between the nodes in both the x, y and z-direction, in three dimensions, is used in a Taylor series expansion. This in order to obtain approximations of the next node parameter value in the grid. Here the capricious parameter value is called ϕ. For example if the calculation starts in the two dimensional node (a, b), the value ϕ in node (a+1, b) becomes:

$$\phi_{a+1,b} = \phi_{a,b} + (\frac{\partial \phi}{\partial x})_{a,b}\Delta x + (\frac{\partial^2 \phi}{\partial x^2})_{a,b}\frac{\Delta x^2}{2!} + (\frac{\partial^3 \phi}{\partial x^3})_{a,b}\frac{\Delta x^3}{3!} \ldots \quad (39)$$

where Δx is the difference between the two nodes.

Similarly the expression for ϕ in node (a-1, b) becomes:

$$\phi_{a-1,b} = \phi_{a,b} - \left(\frac{\partial \phi}{\partial x}\right)_{a,b}\Delta x + \left(\frac{\partial^2 \phi}{\partial x^2}\right)_{a,b}\frac{\Delta x^2}{2!} - (\frac{\partial^3 \phi}{\partial x^3})_{a,b}\frac{\Delta x^3}{3!} \ldots \quad (40)$$

Subtracting equations (39) and (40) along with some rewriting gives the following expression:

$$\left(\frac{\partial \phi}{\partial x}\right) = \frac{\phi_{a+1,b} - \phi_{a-1,b}}{2\Delta x} + O(\Delta x^2) \quad (41)$$

where the truncation error $O(\Delta x^2)$ in some sense determines the accuracy of the approximation and is written as:

$$O(\Delta x^2) = -\frac{(\Delta x^3/3)(\partial^3 \phi/\partial x^3)}{2\Delta x} \quad (42)$$

The equation (41) is called a central difference and is one possibility to approximate the first order derivative. If Δx is smaller, the truncation error's degree will better describe the accuracy of the approximation. This is natural since a smaller distance Δx between the nodes, also gives a smaller truncation error.

Other possibilities for approximation such as the forward and backward difference will not be discussed in this report since they generally have a truncation error that is not so highly dependent on the Δx. This means that they are expected to give lower accuracy. For the interested reader, the book (J.Tu, 2013) is recommended.

2.3.2.2. Finite Volumes

The finite volume method is based on the domain being separated into a finite number of volumes. Interesting parameters are calculated at the centre of the volume and the surface values are then interpolated. An equation for every volume that includes values from bordering nodes can be compiled.

One of the major benefits with the finite volume method is the fact that it doesn't use grid intersection points, since it works with volumes, and therefore can be used for any types of grids. This in

comparison to the finite difference method that needs a somewhat structured mesh. To be able to use unstructured grids can be very useful and gives much more versatility for complex structures.

An essential part of the finite volume method is the volume integration of the derivatives of the generic variable ϕ. With the use of the boundary surfaces A_i^x and A_i^y in the x and y-direction along with Gauss' divergence theorem the integrals can be written:

$$\left(\frac{\partial \phi}{\partial x}\right) = \frac{1}{\Delta V}\int_V \frac{\partial \phi}{\partial x} dV = \frac{1}{\Delta V}\int_A \phi dA^x \approx \frac{1}{\Delta V}\sum_{i=1}^{N} \phi_i A_i^x \quad (43)$$

$$\left(\frac{\partial \phi}{\partial y}\right) = \frac{1}{\Delta V}\int_V \frac{\partial \phi}{\partial y} dV = \frac{1}{\Delta V}\int_A \phi dA^y \approx \frac{1}{\Delta V}\sum_{i=1}^{N} \phi_i A_i^y \quad (44)$$

where N is the number of surfaces in the volume and ϕ_i is the parameter value at that specific surface. These two equations give a very simple way to discretize for example the continuity equation. There is no need to transform the continuity equation to a computational domain since the physical domain can be used straight away. This gives an advantage when it comes to computation time in comparison to, for example, the finite element method.

2.4. Turbulence

Turbulent flow is not strictly defined but is characterized by unpredictability, high Reynold's number and a chaotic flow. There are many possible reasons for turbulence, for example high velocity of the free stream or disturbance in some form.

In order to at least approximately catch the behaviour of a turbulent flow a three-dimensional model is needed since turbulence is characterized by its three-dimensional conduct. Important is also that the turbulent flow consists mainly of eddies which gives an even more unpredictable behaviour.

Because of all these features of turbulent flows it is not possible to resolve it on all different length scales. Special models for calculation is therefore needed. Here, a few of these are mentioned and briefly described.

2.4.1. Near Wall Treatment

First of all, the y+ value will here be shortly presented. It is regarded as the dimensionless distance to the wall and defined as:

$$y^+ = \frac{u_* y}{\upsilon} \tag{45}$$

where u_* is the friction velocity[m/s] close to the wall, y the distance[m] to the wall and υ the kinematic viscosity [$\frac{m^2}{s}$]. The friction velocity is a fictional velocity defined as:

$$u_* = \sqrt{\frac{\tau}{\rho}} \tag{46}$$

where τ is the shear stress [N/m^2] in a layer and ρ is the fluid density [kg/m^3].

A turbulent velocity profile close to a wall is presented in figure 1 and it can be seen that the velocity is lower very close to the wall. The value δ is defined as the distance where viscous effects can be neglected and present are also the different boundary layers. In the sublayer, very close to the wall, the velocity is close to zero and therefore the shear stress from turbulence is very low. It follows from this that the viscous shear is dominant and the relation between the dimensionless velocity $u^+$and y^+ can be written as

$$u^+ = y^+ \tag{47}$$

where u^+ is the velocity u along the wall divided by u_*. This linear relationship holds for $y^+ < 5$.

In the log-layer the relation can instead be written as

$$u^+ = \frac{1}{\kappa}\ln y^+ + B \tag{48}$$

where κ and B are constants. The log-layer is situated in the region of $30 < y^+ < 500$.

Between the log-layer and the sublayer the so called buffer layer is situated. In this layer neither of equations (47) and (48) are valid. However, when $y^+ < 11$ the linear relation (47) can be used as approximation and gives a better result than equation (48). When $y^+ > 11$ the logarithmic relation (48) is a better approximation and therefore used.

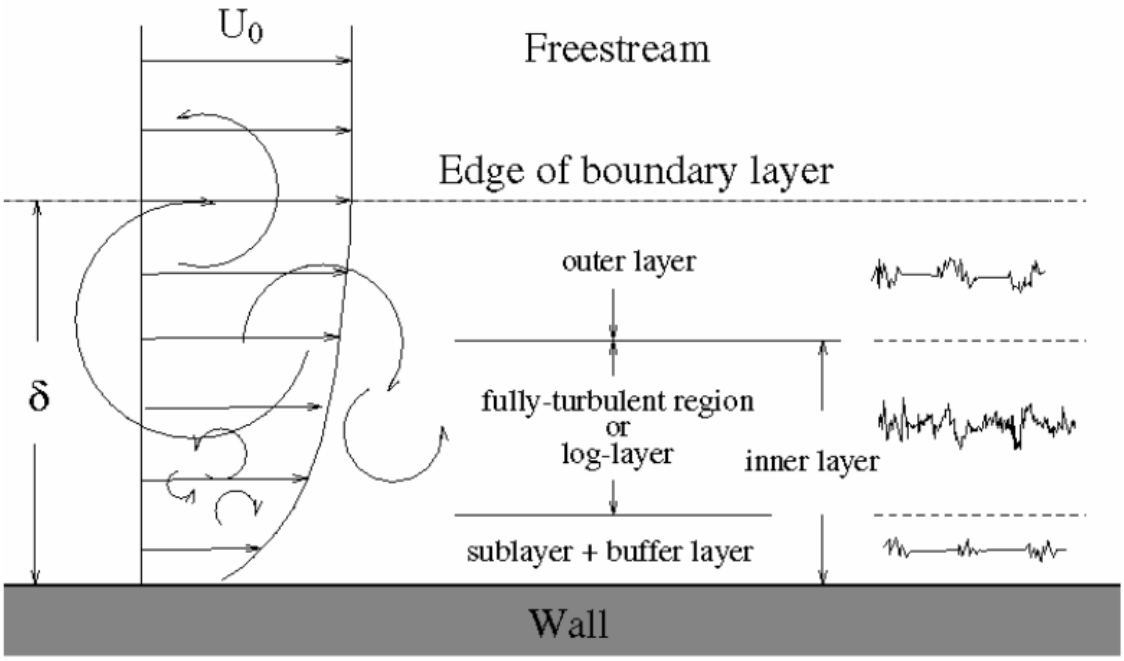

Figure 1, Turbulence velocity profile and layers (V.Mali, u.d.)

Without the use of turbulence models, a very refined mesh would be needed. This since at least some cells would have to cover the sublayer region in order to catch the turbulent behaviour. Therefore a y+ value of around one would be needed since this would approximately mean three cells in the sublayer region, depending on the cell growth rate. However, many turbulence models contain boundary layer models which is why a higher y+ value is often acceptable.

2.4.2. K-ε Model

This method is a very common two equation model. It is numerically stable and robust and is rather accurate for general types of flow. To describe the turbulence it uses two extra transport equations and hence the name "two equation model". The k in the model stands for turbulent kinetic energy $[\frac{m^2}{s^2}]$ and determines the energy in the turbulence. ε is the dissipation rate $[\frac{m^2}{s^3}]$ which is the parameter that describes the rate at which the turbulence kinetic energy dissipates into heat.

Although the k- ε model is commonly used there are some cases where it is not suitable. Examples of these are rotating flows, flows with sudden changes in strain rate and flows over curved surfaces.

2.4.3. K-ω model

As is the case in the k-ε model, the k-ω is a two equation model. Here the k is once again turbulent kinetic energy but instead of the turbulence eddy dissipation, the specific dissipation ω is here used. ω gives the rate at which k is converted into thermal energy per unit of energy, which means that the unit is $[\frac{1}{s}]$.

The advantage of this method in comparison with the k-ε model is its ability to handle near-wall flows. It is more accurate and robust in this sense (ANSYS CFX, u.d.). This is mainly because it needs less refined mesh near the walls. Generally the k-ε model needs a lower y+ value close to the walls due to its need of damping functions. The k-ω has not the same need for this and a much higher y+ value can therefore be used but still give satisfying results near a wall.

The main problem with the k-ω model is that it has difficulties when it comes to handling free jet streams (M.Pavlovich Bulat, 2013).

2.4.4. SST Model

The shear stress transport model is a combination of the k-ω and k-ε models. By combining the strengths from these two models, greater accuracy can be achieved. Close to walls or boundaries, the k-ω is used and in the turbulent and fully developed free stream, far away from the wall, k-ε is used. This is done by a blending function where ε is substituted into ω from the relation $\varepsilon = k * \omega$.

As a summary it can be said that the SST model is widely used in CFX because of its versatility and decent control of the trade-off between different flow regions. This is therefore the method that will be used later in this thesis.

2.5. Multiphase flows

In many flows there is only one phase active. However there are some flows that contain many different phases and an example of this is air bubbles in liquid water. These flows are called multiphase and extra care must be taken to this multiphase phenomenon when modelling using CFD. This is mainly because of the forces acting between the different phases.

Multiphase flows can be divided into subgroups such as gas-solid flows and dispersed two-phase flows. The dispersed two-phase flow is essentially solid particles in a fluid which is actually the case in welding fumes. There you have small, often metal, particles mixed with gaseous phase materials.

Important regarding the dispersed two-phase flow, is the size and concentration of the solid particles, also called the dispersed phase. The particles will collide with each other and be affected by drag forces from the fluid which will make it much more difficult to calculate.

In theory the particles of the dispersed phase are seen as spheres why the particle volume is also the volume of a sphere. This gives that the total volume of the dispersed phase can be calculated if the particle diameter and number of particles are known.

Further problems with multiphase flows in CFD are the complexity of turbulence and various modes of heat transfer. Recommendations for the reader interested in multiphase flows is (M.Sommerfeld, 2008).

2.6. Buoyancy

Buoyancy is the force that acts on a body due to different weights with the help of gravity. An example is a particle that has lower density than the surrounding fluid. Buoyancy can come from a number of different causes. These are for example temperature variations and local pressure variations in a fluid which will alter the density and therefore the buoyancy phenomenon arises. Altering densities in multiphase flows can also be a reason for buoyancy.

2.7. Meshing

Meshing is always of importance in order to achieve convergence and correct results. Typically, a refined mesh is needed close to the walls and in important areas. The reason for this is that it happens a lot in these areas and a more unpredictable behaviour occurs here. Examples of important areas can be high temperature gradient or high velocity areas. Other important areas are where essential measurements and outputs are made. Close to the walls, the turbulent boundary layers makes it even more important to refine the mesh. The y^+ value can here be used as a measurement of the quality and should be low for the cells closest to a wall as mentioned in the turbulence section.

The quality of the elements in the mesh is also of importance. Neighbouring elements that differ very much from each other give problems when calculating the flow. Other important factors are the skewness of the cells as well as aspect ratios, which show the ratio of length and width.

All these factors are significant in order to even achieve a reliable solution in the end. A decent mesh is at least as important as defining the set-up of the problem correctly and can sometimes be the root of a convergence problem.

2.8. Sampling Methods

Design of Experiments is when data point input values are chosen from some kind of decided range. In order to get as much data as possible from as few data points as possible for this, a strategy for placement is needed. There are a large number of methods for this matter but here only the ones later used in the project will be presented.

2.8.1. Uniform Latin Hypercube (ULH)

The ULH is one of the methods for deciding the DOE procedure. It divides the range set into a number of intervals that are equally large. A sample is then taken from each of these intervals. Important for this method is to not use a linear selection and if the first sample is in the third interval, the second might well be in the twentieth and so on. When a sample has been taken from an interval, this interval is closed and no more samples will be taken from that interval. This makes the method very fast. Another benefit with the Latin Hypercube method is that it forces samples close to the boundaries to be chosen. This gives a wider range and less risk to miss certain possible and important sample points.

2.8.2. Incremental Space Filler (ISF)

This method is quite simple and its general aim is to fill out areas with low concentration of data points. The procedure is to identify areas with less concentration of data points which is done through finding the largest minimal distance between two points. In this space a new point is placed and then the procedure starts again and so on. This is a simple method that needs little computational power.

2.8.3. Lipschitz Sampling

This is a method for sampling with the strategy to fill high gradient areas of a function with data points. The procedure for this will here be described.

First of all the Lipschitz constant, $L_{f,D}$, is introduced as

$$L_{f,D} = \sup_{x_1, x_2 \in D} \frac{|f(x_1)-f(x_2)|}{|x_1-x_2|} \tag{49}$$

where x_i is an arbitrary point within the domain D and f is the function response in that point.

If the parameter a is defined as the distance between the two points x_i, the responses' difference cannot be larger than $L_f * a$. This is a useful aspect of the Lipschitz constant, however it does not take into account the curvature of a function ((A.Lovison, 2010)). Because of this, a merit function is needed and is defined as

$$merit\ (x) = L(x) * Radius(x) \tag{50}$$

where x is an arbitrary point within the domain, L(x) is the estimated local Lipschitz constant and the Radius is the distance from x to the closest data point from the starting set of data. This merit function then becomes a measurement of the curvature since the Radius shows how far away the next data point is.

The procedure of the Lipschitz sampling is to have a set of data points, find f(x_i) for each of these data points and then estimate the Lipschitz constant in a region around an arbitrary point x. After this the merit function can be calculated and then the regions with the highest merit values are considered in need of more data points since the gradient is high here.

2.9. Optimization Methods

There are a number of methods used for finding the optimum in a set of data points. Used for this project is however only the so-called MOGA-II with the help of a response surface.

2.9.1. MOGA-II

MOGA stands for multi-objective genetic algorithm and is used to find the optimal point in a set of data. MOGA-II is a development of MOGA with the aim of solving potential errors with this method (S.Poles, 2003). The method is based on elitism where the best points are to be used. At first an elite condition is set and evaluation on which data points the elite region contains is performed. These points are then used to form a new data set with the aim of combining the best designs. The new data set is then formed into another elite region. This new elite region is then set as the standard region and another elite condition is developed, along with new evaluations of points and so on. The aim of this is moving closer and closer to the optimum and eventually find it. In this method it is also used that some points are placed in other regions in order to reduce the risk of missing a potential optimum.

2.9.2. Response Surface

A response surface is generally a function made from a set of data points through the use of a mathematical method such as kriging. Kriging uses interpolation between the data points to obtain values in the empty spaces. These mathematical methods will however not be further investigated in this project.

Instead of running simulations with many data points, which cost computational power, a response surface can be built and optimization can be done on the response surface function instead. This can save a lot of time and is therefore often preferred.

2.10. Pearson Correlation

This is a method for deciding correlation between different parameters from a set of data points. Three different cases could occur for Pearson correlation of parameters. Namely positive correlation, negative correlation or no correlation. The method also calculates a coefficient for measuring the size of the correlation. This coefficient is called the Pearson coefficient and is a value between -1 and 1, where -1 is negatively correlated and 1 positively correlated.

The problems with Pearson correlation is that it does not take into account that both parameters do not have to be correlated just because one of them rises while the other rises. An example is if the correlation between smoking and an early death where smoking could lead to an early death and so is correlated with that. However, an early death does not lead to smoking which is what the Pearson correlation shows. As a researcher, this must be taken into account.

3. Introduction to Modelling

This chapter will mainly describe the general setup and methods used for calculating the flow. The software used is ANSYS CFX along with ANSYS DesignModeler, for geometry construction, and ANSYS Mesh for meshing. The project is divided into several cases where the first case is the physical phenomena testing and the second one the verification case used for verifying the model. More cases are the different types of welds, namely MIG, TIG and SMA along with the parametric testing case. Additionally there will be a final optimization case of the so called on-torch suction. In this section, the general approaches that do not differ too much between the cases will be presented.

3.1. Geometry

Although some parts of the different geometries are similar, the geometry is considered case particular and will be described in detail at each case section. Figure 2 describes the geometry of a three dimensional MIG weld, however all cases have been built up in a similar way. In all cases there are some kind of a handle (purple area in figure 2) which is mostly considered a wall with fixed temperature. This means that the handle will not be meshed which saves time during the calculations. All cases also have a workpiece which in figure 1 is infinite and represented by the orange area. This is considered an interface between solid and fluid which can lead heat and is therefore not adiabatic.

The domain is also general and divided into a solid and a fluid part. In the fluid domain, the outer boundaries are constructed as openings with atmospheric pressure which allows fume and other gases to pass. This makes it possible to have a smaller domain but still achieve correct results which is beneficial since the room where welding takes place is considerably larger in reality, than the domains used in this project.

All geometries in the different cases also consists of some kind of electrode (white part in figure 5) although its geometries differ. There is also a warm part (red area in figure 5) which in reality is the lowest part of the electrode.

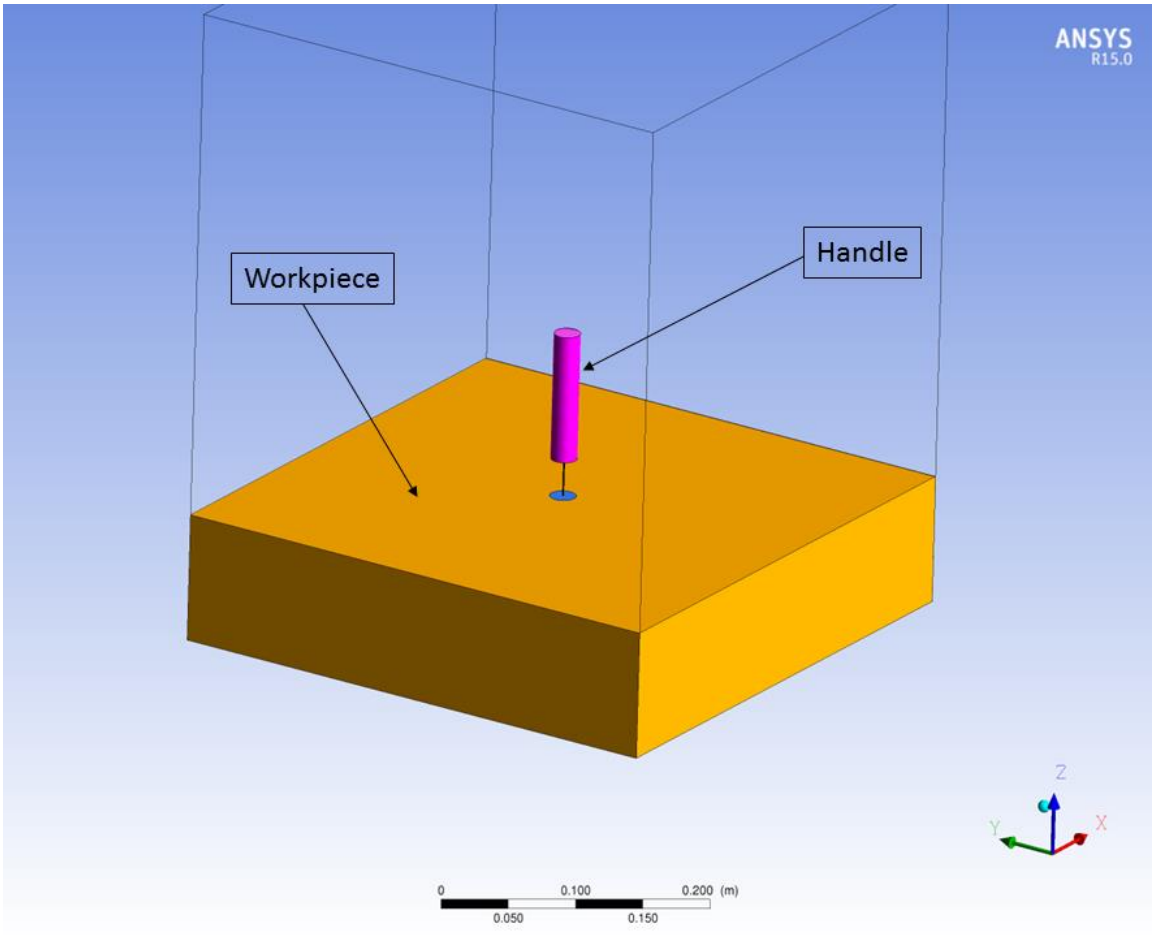

Figure 2, General geometry of the welding

3.2. Meshing

The meshing is of course case specific, however the strategy for meshing is similar. As mentioned in the theory section, the important parts are close to the welding heat release and close to the interfaces between solids and fluids. These areas are always inflated and refined in order to obtain correct results. It is important to have small y+ values here, preferably close to one, because it is needed to catch the turbulent behaviour of the flow sufficiently. The mesh quality is also important in these regions but has not been prioritized in other regions. To have a detailed mesh must always be weighed against the fact that the calculations should be fast. From this it follows that a less detailed mesh in unimportant regions is a well approved strategy.

Figure 3 shows the mesh of the two dimensional verification case which will be presented in detail later. Only parts of the mesh can be seen and notable is that there are refinements close to the workpiece since this is modelled as a wall in this case. There are also refinements close to the handle and in figure 4, which shows a close up of the area around the electrode, it can be seen that there is also a refinement close to the electrode. Notable is also that the general size of the cells in the area around the electrode is quite small. This is due to the fact that there are both fume release, shield gas release and heat release in this area. All these releases will create an unpredictable behaviour and therefore needs a finer grid.

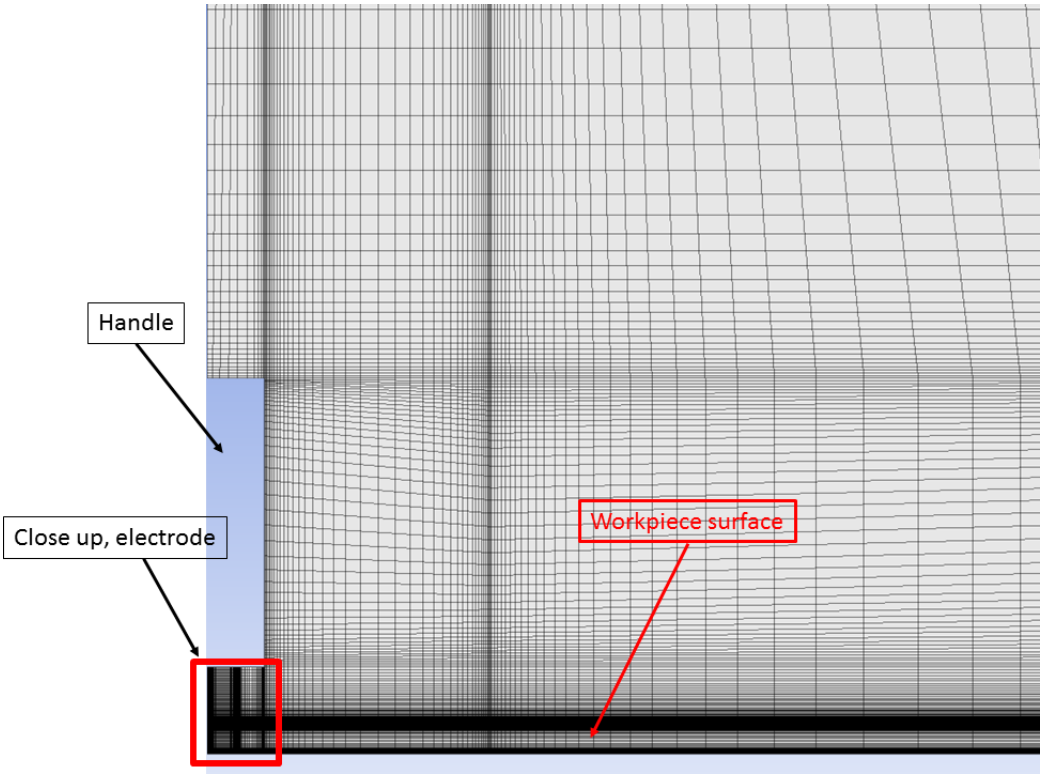

Figure 3, Part of the verification case, mesh

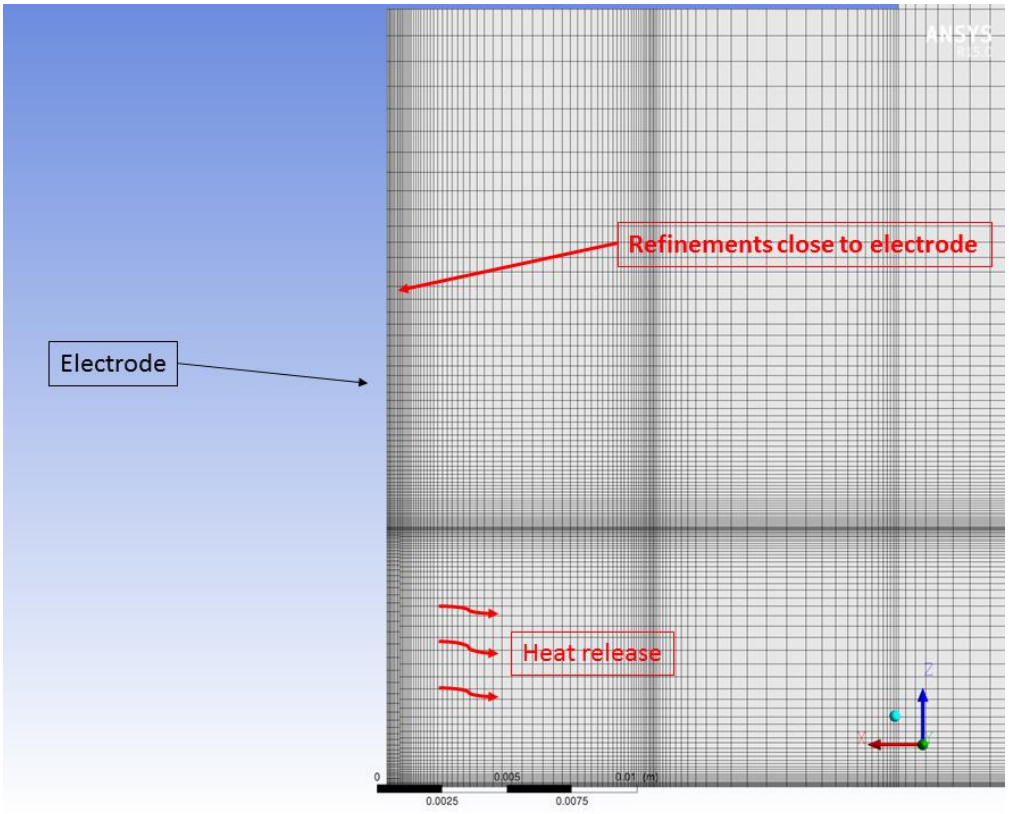

Figure 4, Close up of verification case, mesh

3.3. Setup

Regarding the setup, the fume release, shield gas rate, heat release and many other parameters varies in the different cases. Nevertheless, there are similarities here as well. For example, the fluid domain will always be set to contain air and room temperature as initial conditions. The amount of fume released will be set from experimental values. Direct electrical current will always be assumed in this project and will be used to calculate the heat release from:

$$P = U * I \tag{51}$$

where U is the voltage [V], I the current [A] and P the effect [W].

It is also assumed that all electricity is released as heat from the warm part at the bottom of the electrode (red part in figure 5), since there are only tiny losses on the way in the electrode and other parts. The fume will then be heated by this heat release when it passes. Important for the heat transfer will be the radiation which will be calculated using the discrete transfer method. This since it is a quite fast method with good enough accuracy. Notable is that the radiation is only calculated every tenth timestep on the transient runs. For the other timesteps an old value is used. The reason for this is to get a faster model that is still accurate enough. That the accuracy is not affected too much has to do with the fact that the radiation is not so strongly correlated with the flow parameters. If this method were to be used with for example the velocity, a divergence problem would probably emerge.

Regarding the fume, material properties will be taken from (Engineering toolbox, u.d.) and it will be released from an area that represents the molten part of the workpiece (blue part of figure 5). Sizes of this area will vary in the different cases and is set to a real case size. However it is notable that the size of the melt is dependent on many variables in reality but here only one size is assumed.

The fume is set as a dispersed fluid where the metal particles released are small enough to be considered a fluid that has a viscosity similar to an ideal gas. Notable is also that it is assumed that the minor fume components will not be taken into account in the model. The shield gas will be released from the lower part of the handle (green part of figure 5) and will be set at room temperature. Notable for the shield gas release is that the release will differ a little when it comes to the SMA welding. This will be explained deeper in that section but it will generally be released from the warm part instead. It can also be said that the amount of fume released is taken from experimental values and in the cases where the geometry is not entirely three dimensional, the amount released will be scaled. This scaling will be based on the release area size where it is assumed that an equal amount of fume is released over the entire area.

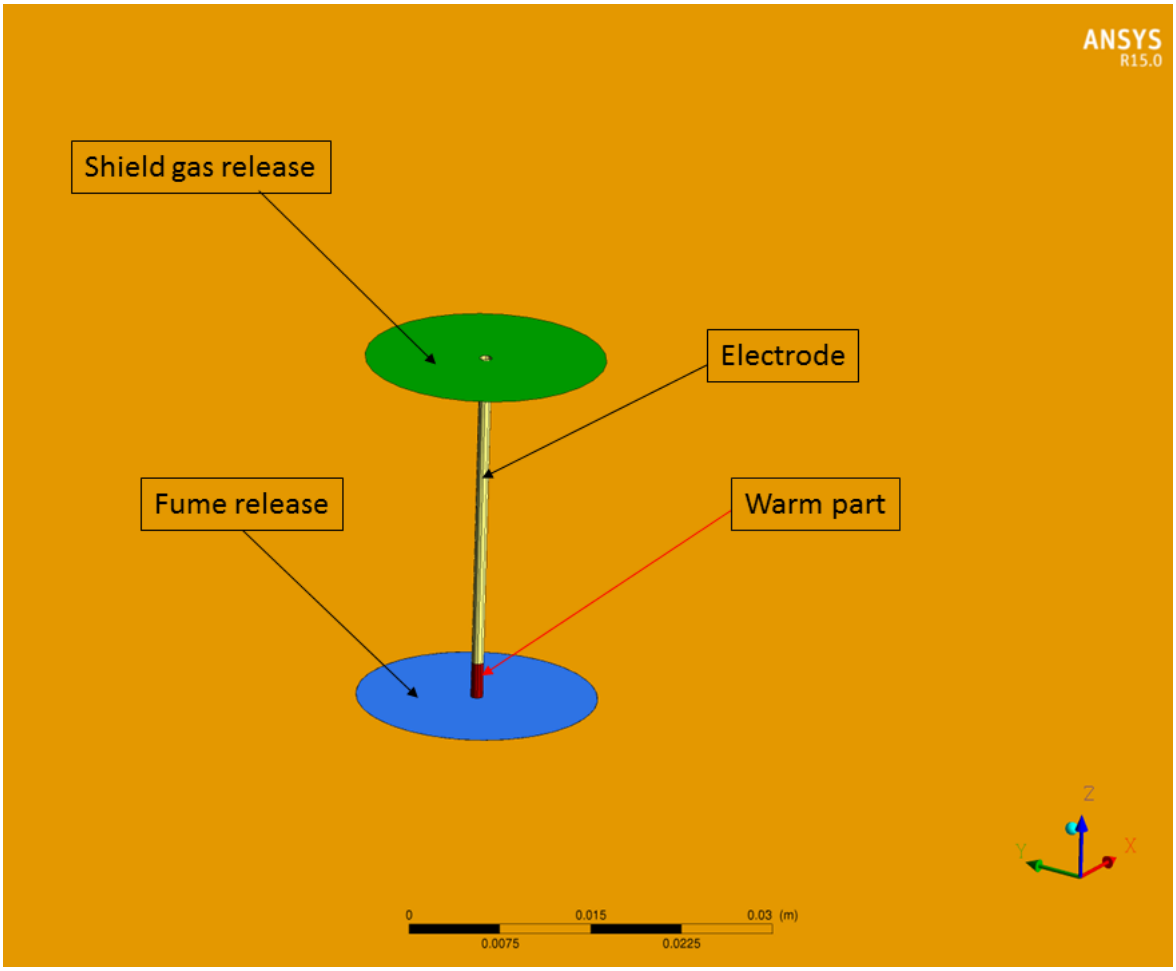

Figure 5, Close up of weld geometry

When it comes to turbulence, the chosen model for all cases is SST (see theory section) since it is a versatile model that works both close to walls and in the free stream. Buoyancy is considered important since it is known from experiments that the welding fume will have a different density in comparison with the surrounding air. It is also expected that a high temperature will be obtained which will enhance the change of density and therefore make buoyancy even more important.

Finally, most of the simulations have been done using a transient setup. Transient conditions are needed in this project because of the high temperature that creates an unpredictable behaviour of the flow. Steady state conditions would in many cases of this project make the solution diverge due to its more inexact calculations based on additional assumptions. The aim of this project is partly to create models that work for many different kinds of values on heat release, fume release etc. This makes it important that the model works for all cases which is not the situation with steady state simulations.

4. Physical Phenomena Testing

Before the final set-up was established a number of tests regarding physical phenomena were performed. This is an important part since it gives an idea of which parameters that can be omitted in the final setup. It is also important for this project in order to establish what parameters that can be expected to have large impact on the fume flow. This will give an idea of which parameters that are interesting to vary in the parametrization case. Extra care have been taken to make these models very fast which of course means that they are less accurate. Still they can give a good enough approximation of the results.

4.1. Radiation

The radiation parameter in the heat transfer was expected to be of importance since the welding temperature is very high. However, radiation is quite costly to calculate when it comes to time and it was therefore necessary to examine the impact of this parameter. It was simply done by using a two-dimensional MIG model with area scaled input values.

4.1.1. Geometry and Setup

As can be seen in figure 6, the geometry consists of a welding handle (2), an electrode (1) and a workpiece (3). All these parts are not meshed and are considered walls apart from some small areas. These areas are the inlet of carbon dioxide as shield gas at the handle (4) along with the inlet of fumes from the workpiece (5). All input heat release is situated at the bottom of the electrode flowing in both positive and negative x-direction. The domain is constructed with the outer boundaries as openings.

Important parameter values such as the fume release (R.F.Heile, 1975) and shield gas rate (Netwelding, u.d.) are presented in table 1. These values are scaled from the three dimensional case with the area of release as foundation. This gives that the values are roughly a percent of the three dimensional values in this case.

Table 1, Setup parameter values of radiation testing

Current, unscaled [A]	200
Voltage, unscaled [V]	30
Heat release [W]	60
Shield gas rate[kg/s], 100 % CO2	4.01e-6
Iron release [kg/s]	2.10e-8
Manganese release [kg/s]	3.17e-9
Oxygen release [kg/s]	1.02e-8
Silicon release [kg/s]	1.22e-8

Finally, in order to get a better result this case was performed with transient conditions, during a period of 2 seconds.

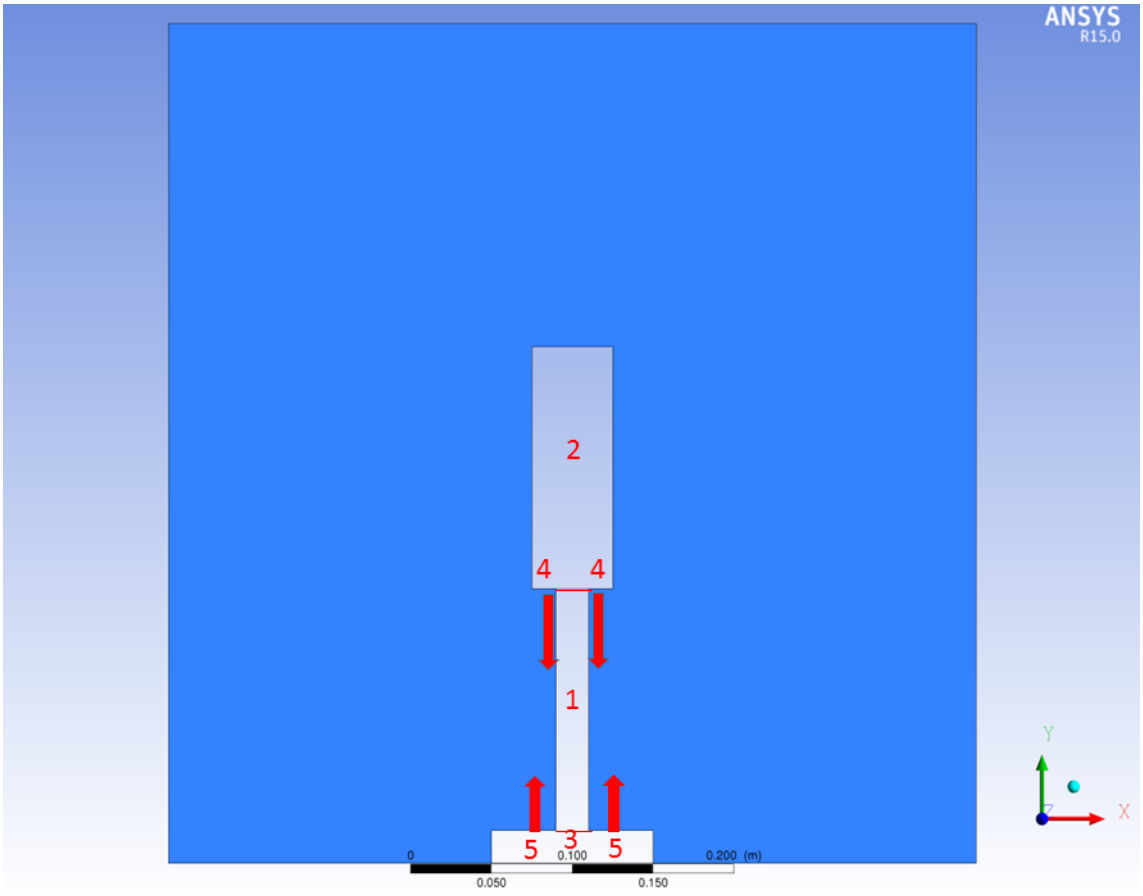

Figure 6, Geometry of radiation testing case

4.1.2. Results

The results from this brief test was very clear. At first the case was tested without any impact of radiation and then the exact same case was tested with radiation impact. The temperature of the domain was then evaluated. In the first case, without radiation, it can be seen in figure 7 that the temperature is not changing much at all. No part of the domain has reached more than approximately 2500 K and the heat transfer is slow.

In the second case however, the radiation shows to have a large impact since it is here obvious from figure 8 that the heat transfer is much quicker. The high temperature has now spread through almost the entire domain and it is also warmer close to the heat release area. Notable is that the cold part right beneath the handle is the room temperature shield gas cooling the domain.

The conclusion of this is that radiation needs to be taken into account.

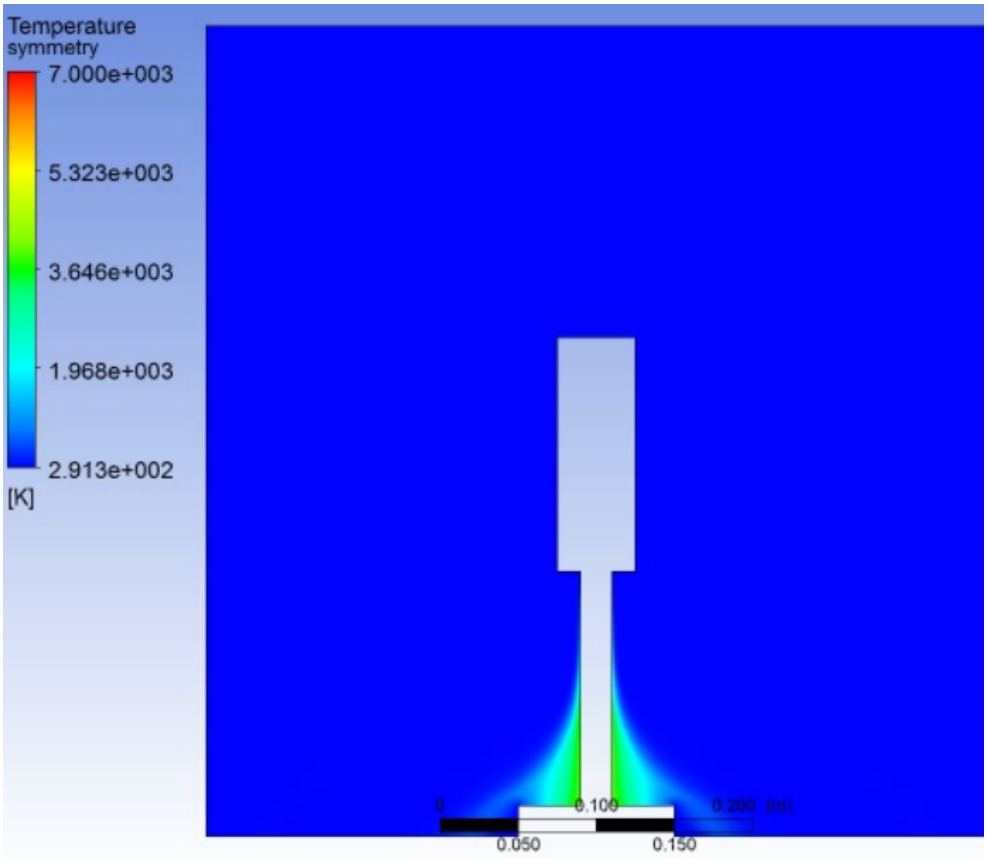

Figure 7, Temperature [K] of the non-radiation test

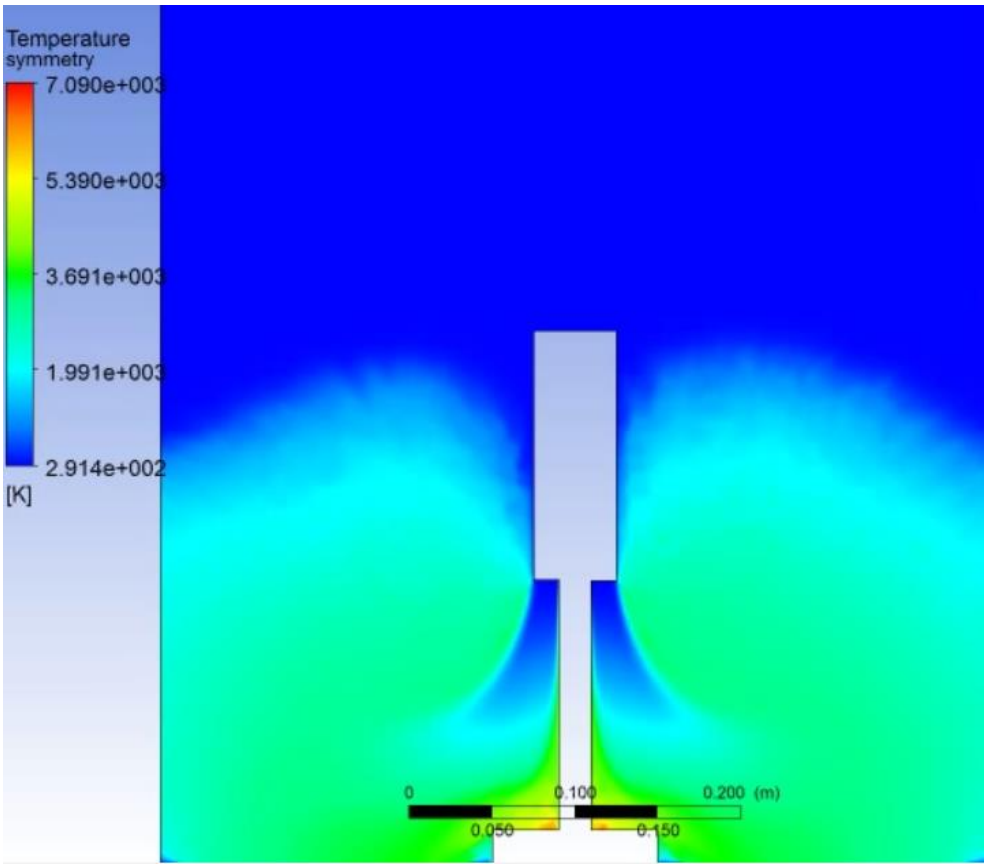

Figure 8, Temperature [K] in the radiation case

4.2. Thermal Conductivity

In this case the thermal conductivity of the electrode and workpiece material was altered in order to simulate how large impact the change of welding material would have on the fume movement and temperature of the fluid.

4.2.1. Geometry and Setup

The geometry and setup are very similar to the case with radiation testing. However one major difference is needed. Since the solid materials of the electrode and workpiece are going to be tested, these also have to be taken into account and meshed. This means that they are no longer treated as adiabatic walls but as solid-fluid interfaces where heat transfer is allowed.

4.2.2. Results

Figure 9 is showing the iron mass fraction from a case with a very low thermal conductivity while figure 10 shows the iron mass fraction from the same case but with the thermal conductivity of steel. Iron is one of the major components in the welding fumes for this case (see table 1) and therefore gives a good look of the fume as a unit. If these two cases are compared there are no essential differences. The difference in mass fractions are small and the movement is approximately the same. This means that the thermal conductivity is not too important and when parametrizing certain values, this is not the most important value to be taken into account.

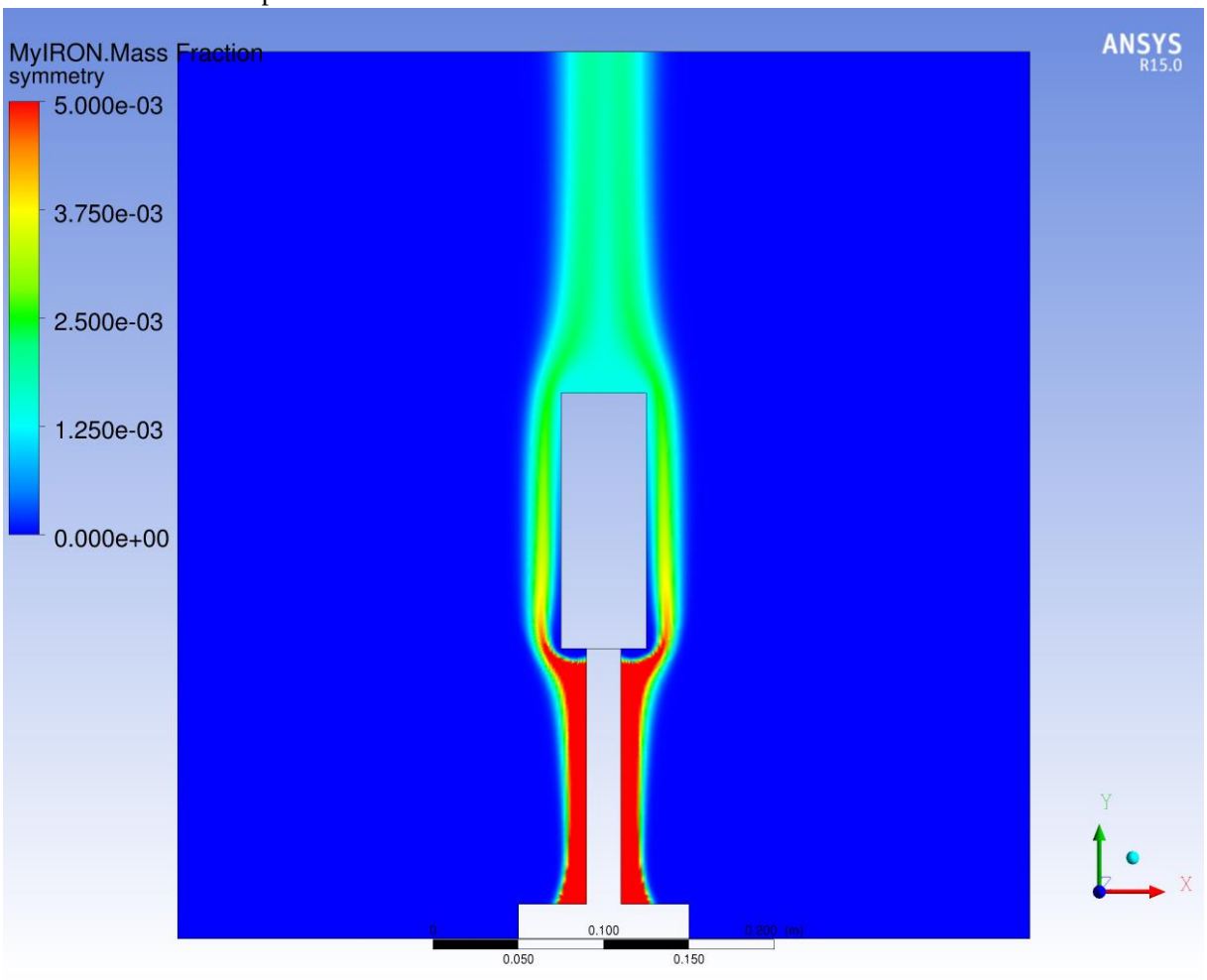

Figure 9, Iron mass fraction when the thermal conductivity is low

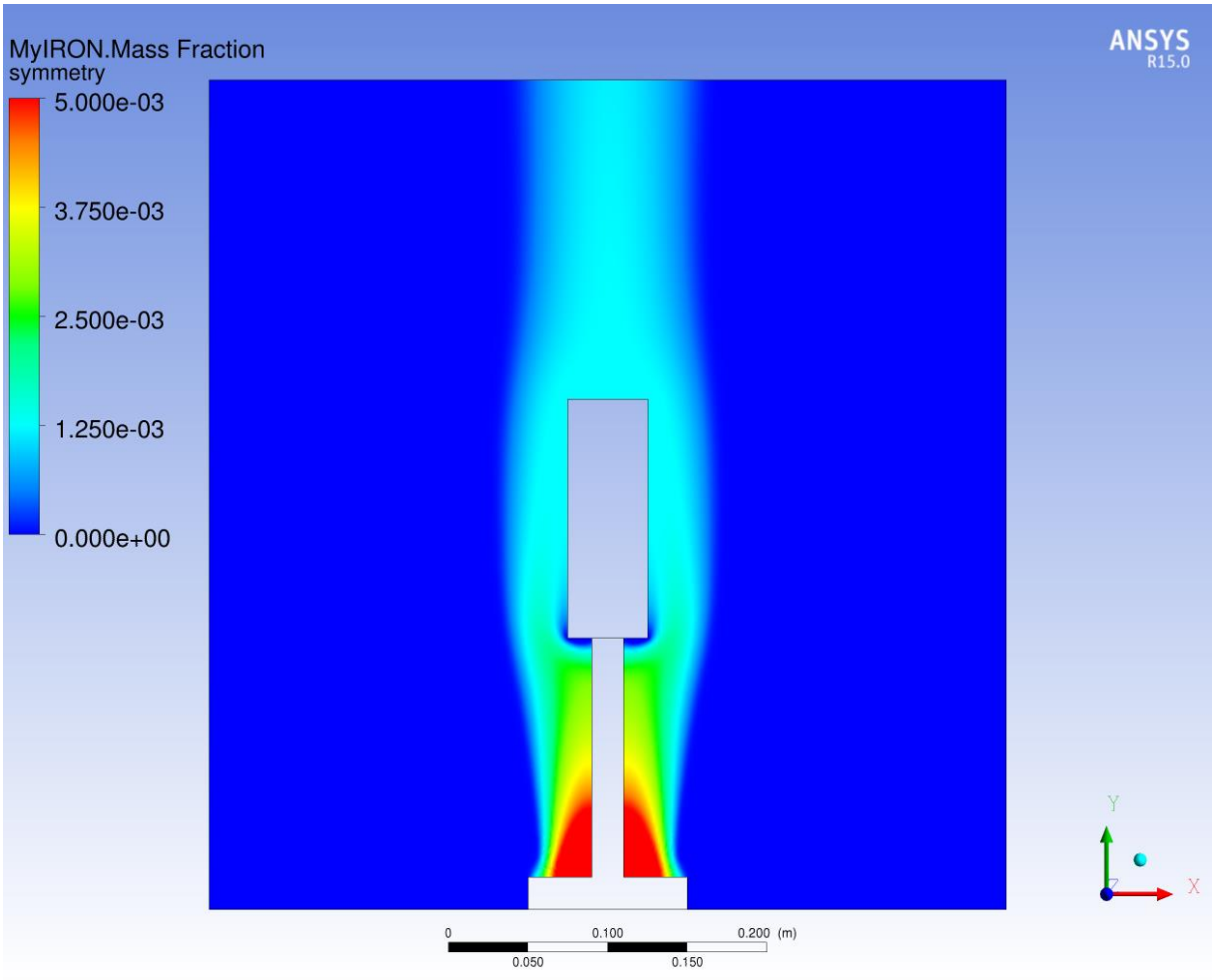

Figure 10, Iron mass fraction with steel thermal conductivity

4.3. Tilted Weld

To alter the angle of the weld is something that is very common among welders. This in order to be able to aim and get access to all parts of a workpiece. It is expected that the fume movement will differ with this since the shield gas flow is changing direction.

4.3.1. Geometry and Setup

The only changes in geometry and setup compared to the previous thermal conductivity case is that we now have a narrower electrode along with an infinite workpiece. This makes the model simpler and easier to calculate. It is also closer to a real welding case with the narrower electrode. The model has also been improved to a more realistic one through the use of a moving electrode which is the case for an actual MIG weld.

4.3.2. Results

It can clearly be seen that the fume has changed direction in figure 11. This is probably due to the flow of shield gas as mentioned before. The shield gas is pushing the fume in a certain direction due to altered angle. However, it must be taken into account that this is a two dimensional model which means that the different gases cannot flow past the handle or electrode. This will of course affect the result and is possibly the reason that the fume flow is not continuing straight up after the handle.

Although this case does not show entirely correct results, it shows that the welding angle is of importance which is valuable to know for the parametrization case.

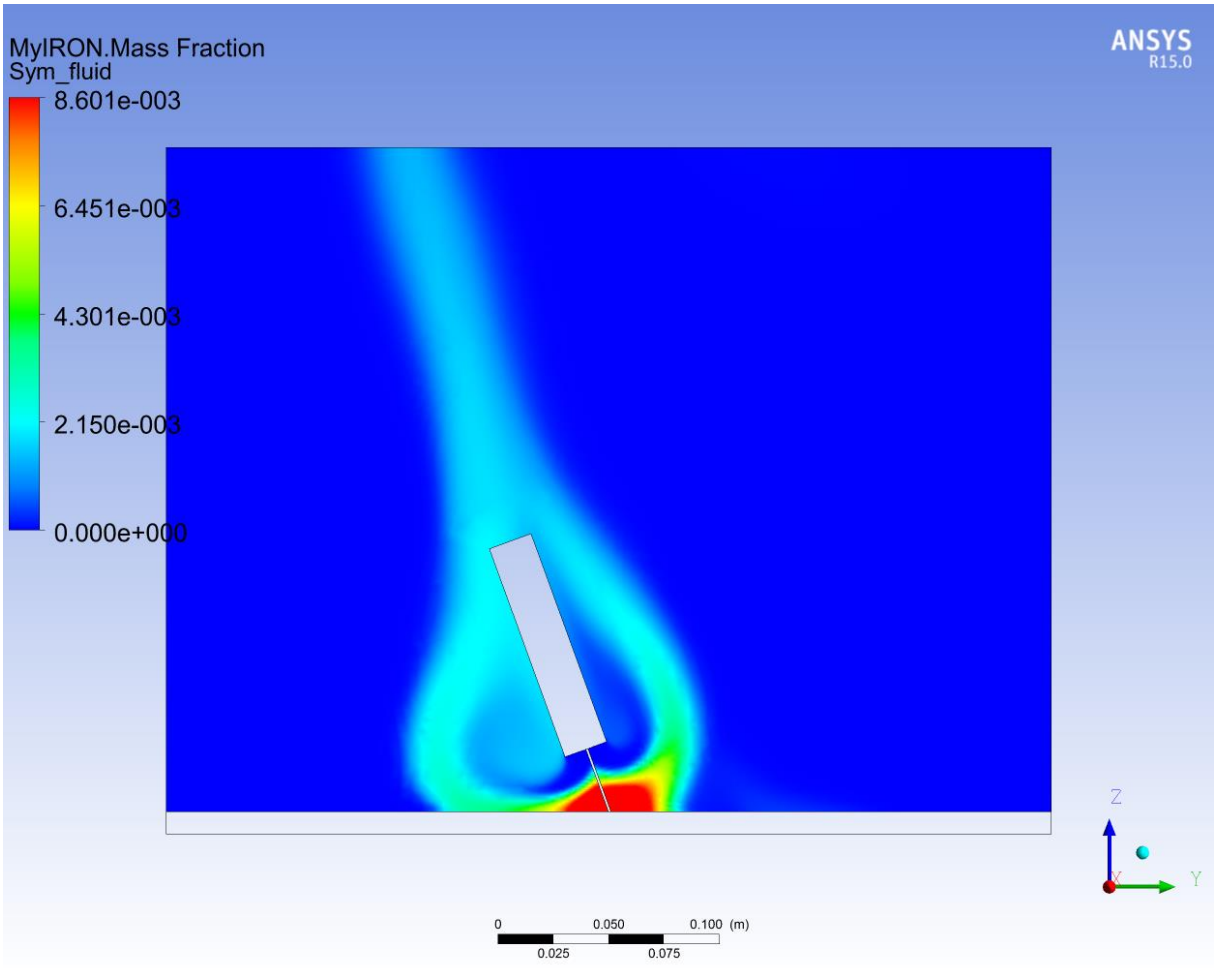

Figure 11, Iron mass fraction of tilted weld

5. Verification Case

In order to validate a model, a verification procedure is needed. In this project a model is built up and evaluated from experimental results measured at Lund University in the late 1970s (K.Malmqvist, 1980). These experimental results will here be referred to as the Lund-case. Used for validation is the fact that the particles are homogenously gathered in the filter in these experimental results (K.Malmqvist, 1980).

The chosen welding method here is MIG with a current of 200 A and a voltage of 30 V. This gives a heat release of 6000 W. The shielding gas used is pure carbon dioxide and the electrode –and welding material is steel. Feed rate of the wire is set to 10 m/min which is a quite normal value (Foremen Training Institute Bangalore, u.d.)

5.1.1. Geometry

In order to make a faster model, the geometry (see figure 12) is split up into a two dimensional axisymmetric piece of 10 degrees with an aluminium shell shaped as a horn. At the top of the horn, a fan is situated (5 in figure 12) which sucks air from an open lattice at the bottom where the weld is also located (4). The weld is surrounded by a curtain (3) in order to prevent the fume from evading. A Millipore AP 2529325 filter, that catches particles, is situated right at the pointy swell close to the top of the structure (1). A pipe (2) with solid walls is leading the fume to this filter.

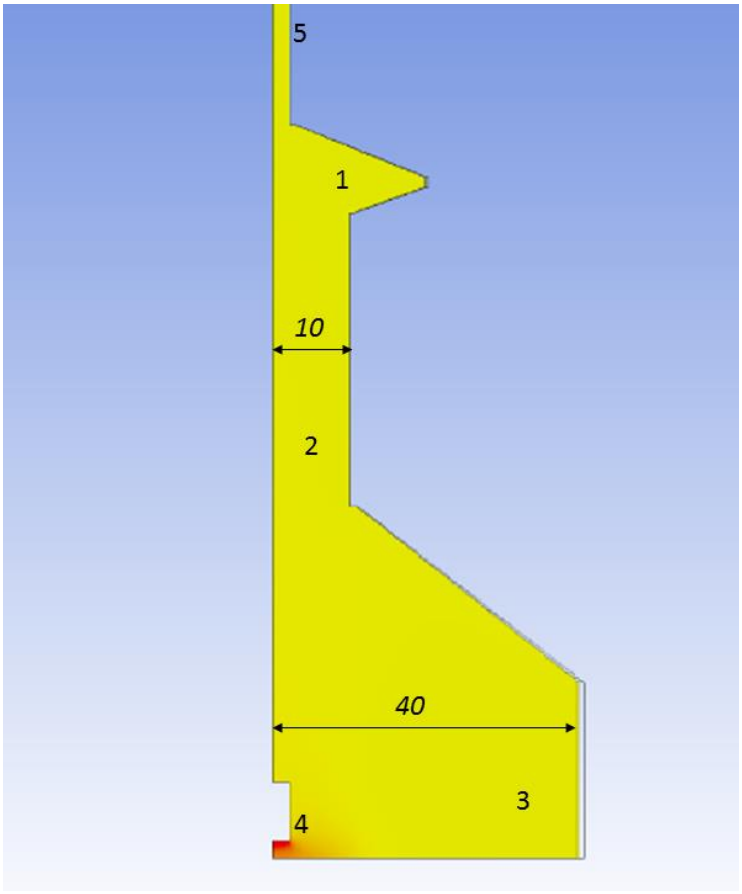

Figure 12, Geometry of verification case, distances in [cm]

5.1.2. Set up

In order to verify the model, the same set up that will later be used in the real cases must here be utilised. Used in this set up is another experimental case (R.F.Heile, 1975) also used in the previous

chapter and here referred to as the 1975-case since that is the publication year. A case with the same electric current and voltage as the Lund-case has here been found and then the fume release from this case has been used. The fume released consists mainly of manganese, iron, silicon and oxygen (see details in table 2) and is scaled as 1/36 of the real value due to that the geometry is an axisymmetric piece of a three dimensional structure.

Table 2, Verification case gas release, scaled values

Particle material	**Amount released [kg/s]**
Iron	5.85e-8
Manganese	9.1e-9
Silicon	3.38e-8
Oxygen	2.86e-8
Shield gas, pure CO2	1e-6

This case is run in steady state until convergence has been achieved. The filter is modelled as a fall of pressure over that certain filter region. This pressure fall corresponds to an air resistance of 35 mm water (Merck Millipore, u.d.) measured with a water flow of 0.053 m/s.

5.1.3. Results

The desired results would be a homogenous distribution of fumes in the filter since this would show that the model is accurate. In figure 13 it can be seen that this is the case. There are differences in the iron mass fraction but these are so small that they are negligible. The fact that there are differences is in fact positive. This since if there were not, it would show that there are no differences at all in the pipe flow which of course would not be realistic. The difference between the highest and the lowest mass fraction in the filter is approximately 3e-5 which is 0.2 % of the maximal mass fraction in the filter. In the report (K.Malmqvist, 1980) the result is a homogeneity of 3 % which is considerably larger than 0.2 %.

From these results, the conclusion that the model used is verified can be determined. Since no other measurement data was available and due to the fact that the main goal for this thesis is not exact verification, it was decided that one verification case is enough. To get an even more accurate model, more verification cases could be evaluated.

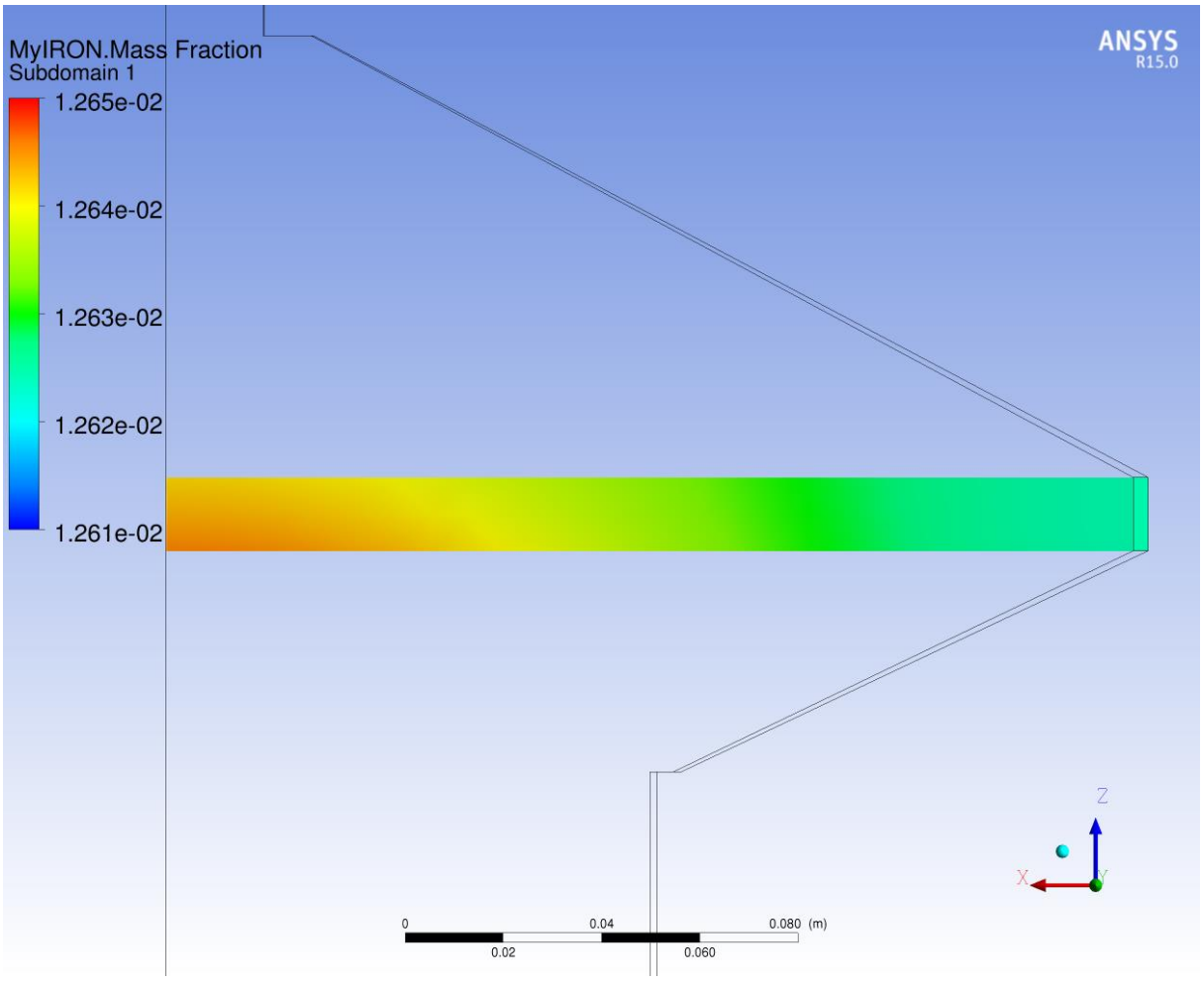

Figure 13, Iron mass fraction at filter

6. Three Dimensional Welding

The cases presented in this chapter are the three dimensional weld models built up to simulate the actual behaviour of the different gases and fumes. These models are built with the purpose of, in the future, being used for tests and evaluations of the gas and fume behaviour. The results from this will mainly be the actual models and the fact that they are working and are accurate enough.

6.1. MIG (Metal Inert Gas)

MIG welding has already been discussed earlier in this report and is one of the most common methods. It is also considered the main welding method for this thesis. The MIG relies on a shield gas flow in order to keep the molten part protected from the air.

6.1.1. Geometry

The geometry is very similar to the one described in the Introduction to modelling-section with a vertical handle. Regarding the size of the geometry it is quite small in comparison with the size of a human body or a room where welding takes place. Exact dimensions, apart from electrode diameter (1 mm), can be seen in figure 14 and figure 15. The reason to use a smaller room although it would be interesting to know what happens far away, is the fact that a large domain takes much computational power and time. This smaller geometry still captures the behaviour adequately and conclusions can be made of where the mass fraction of fume is high.

Three different domains are used, namely the moving solid (see figure 14), the solid and the fluid (see figure 15). The moving solid contains the electrode and the warm part and is moving with the constant speed of 10 m/min straight downwards. Only one part is in the solid domain, namely the workpiece. The fluid domain consists of the room initially filled with 298 K air.

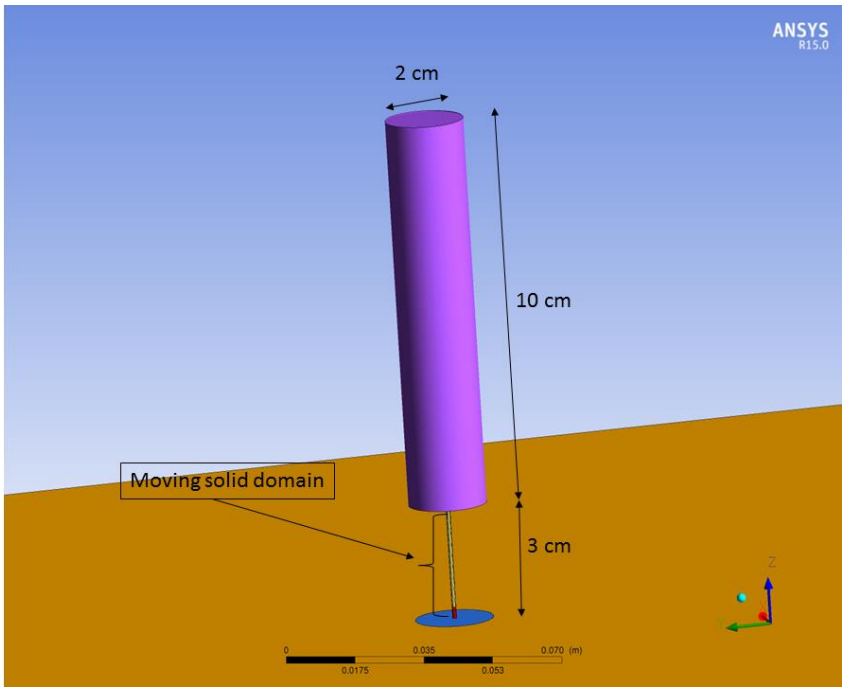

Figure 14, MIG weld geometry

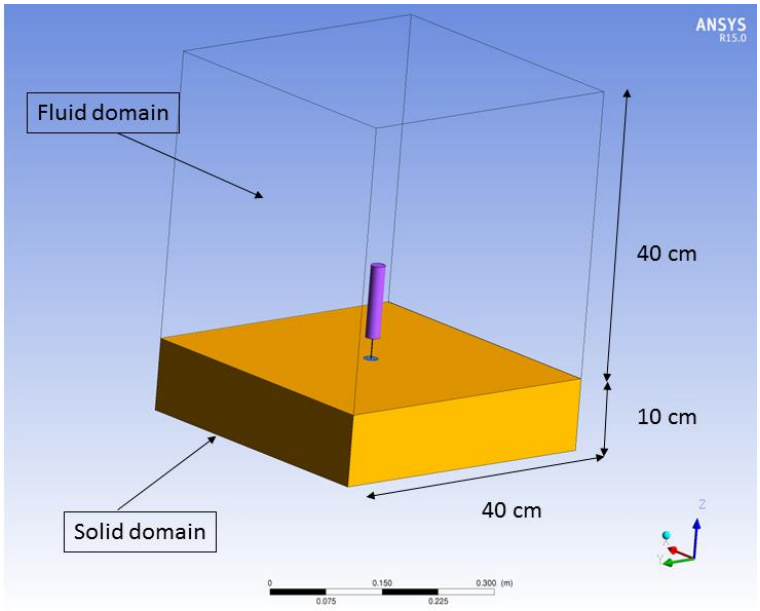

Figure 15, Entire MIG geometry

6.1.2. Setup

The simulation is run transient for about 0.8 s which is chosen in order for the fume to reach a sufficient height to be evaluated. The shielding gas used is pure carbon dioxide and the fume consists mainly of iron, manganese, silicon and oxygen. The release of these gases will be the same as described earlier for the general case. Table 3 shows the exact release rate of the different gases where the fume composition is taken from (R.F.Heile, 1975) and the shield gas rate is set to a common value for MIG welds (Netwelding, u.d.)

Table 3, MIG gas release rates

Iron [kg/s]	2.1e-6
Manganese [kg/s]	3.16667e-7
Silicon [kg/s]	1.21667e-6
Oxygen [kg/s]	1.01667e-6
Shield gas, 100% CO2 [kg/s]	3e-4

The electric current is 30 A and the voltage 200 V which will give a heat release of 6000 W from the warm part.

6.1.3. Results

From the simulations of this three dimensional MIG weld, some different results were obtained and evaluated. The flow of fumes is shown in figure 16 where mass fraction of iron, that is one of the major fume components, is plotted in a centred plane that goes through the middle of the weld. Notable in these results is that the fume is affected by the shield gas flow which is why the flow direction is outwards from the electrode at that region. Then the heat from the weld makes the fume density become lower and the fume rises.

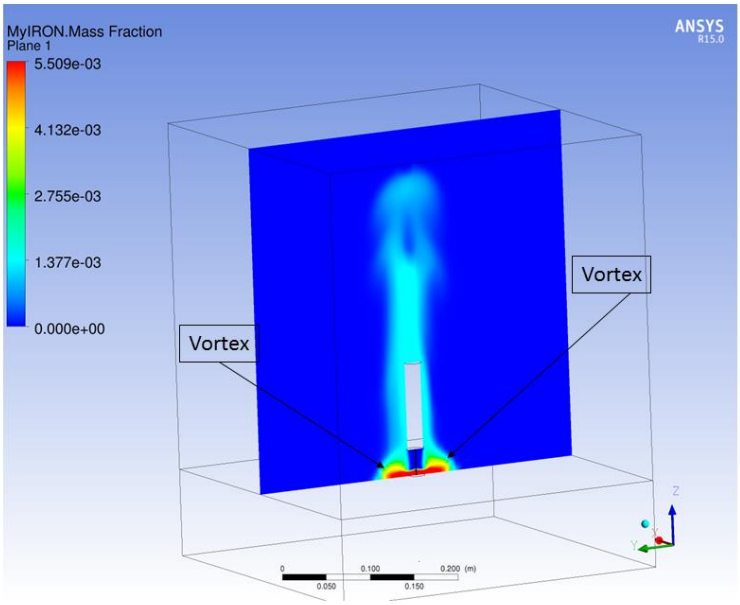

Figure 16, Centred plane showing iron mass fraction

Interesting is to see the flow over time more clearly. This is shown in figure 17 where the rise of fumes can obviously be seen from three different positions of time.

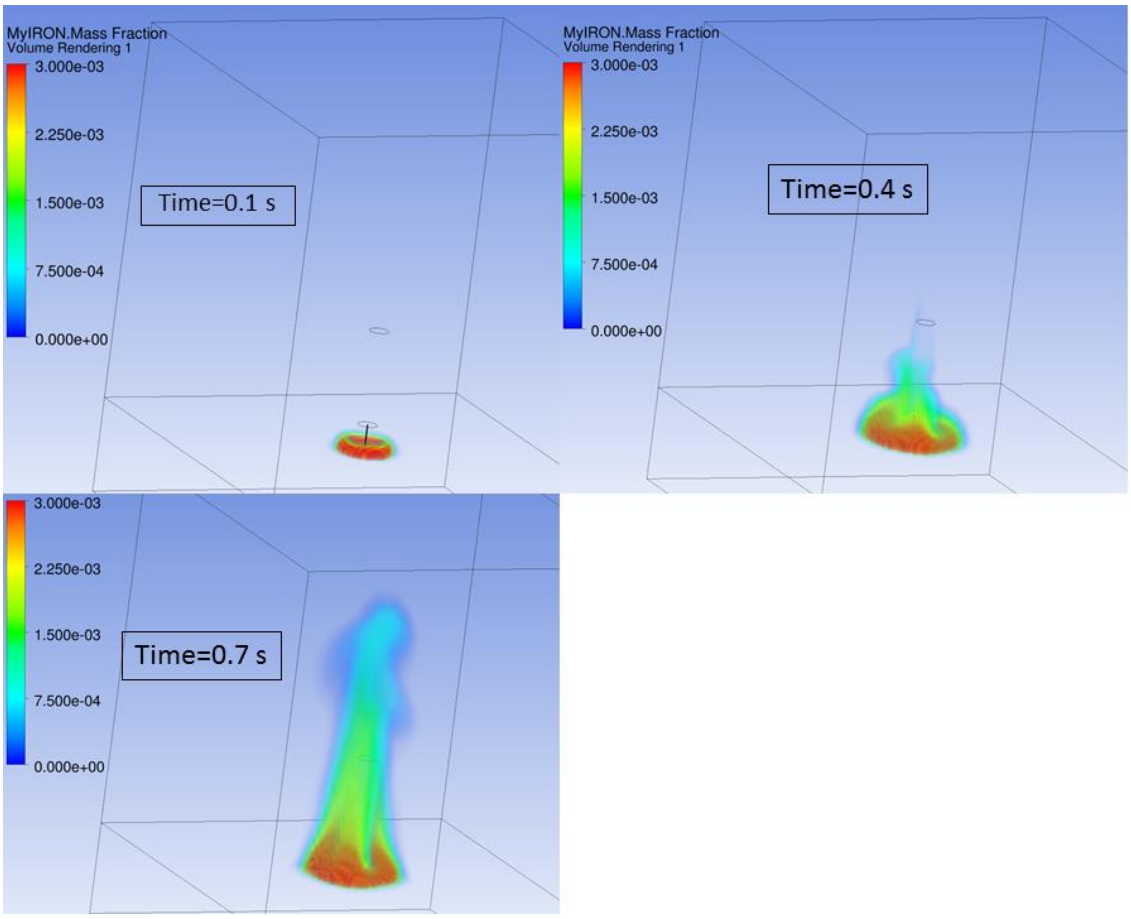

Figure 17, Mass fraction of fumes at three different times

The shield gas also makes vortices appear in the flow through its flow downwards which can clearly be seen in figure 18. This shield gas flow collides with the fume flow making the flow direction outwards from the electrode (see figure 18). The reason that the fume is later aiming back into the middle is probably that the shield gas flow draws air downwards. This creates an empty space which will then be filled by fumes and therefore a vortex is created.

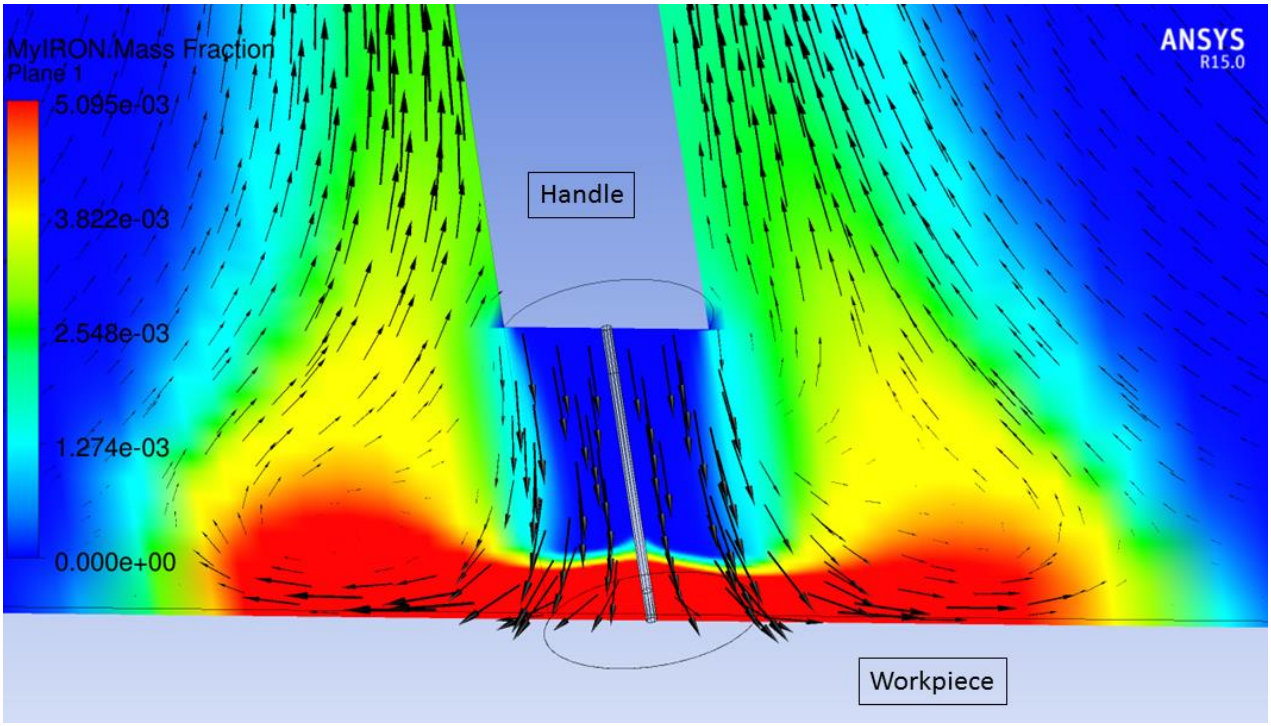

Figure 18, Velocity vector field showing close up of the vortices

The three dimensional behaviour of the fume and shield gas flow is captured well in figure 19. Here velocity streamlines has been drawn to easily see the direction of the flow and the fact that the gases are flowing all around the handle. The unpredictable behaviour of the gases in the vortices shows that a three dimensional geometry is needed. A two dimensional geometry does not allow the fumes to flow past the handle and electrode which could possibly happen, as shown here.

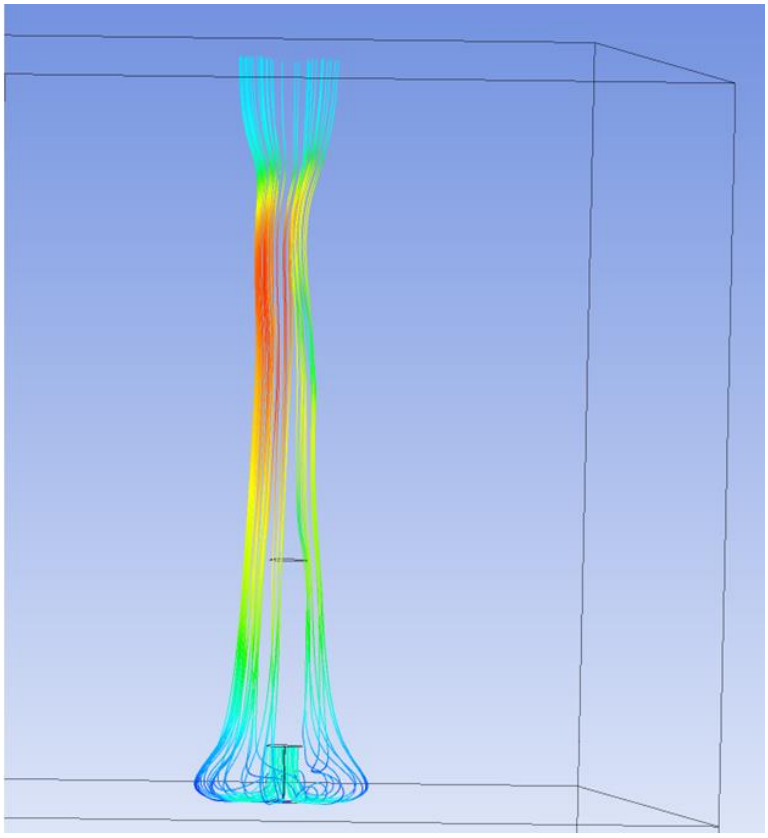

Figure 19, Velocity streamlines, showing 3D effects of shield gas and fume flow

Regarding the shield gas, it is necessary that it covers the molten part (where the fume is released) in order to protect it from the surrounding air. Figure 20 shows that this is obtained with an apparent protective layer along the electrode and around the melt with a mass fraction of roughly 100 %.

A final interesting aspect is the temperature, which can be seen in figure 21. Notable is that the high temperature at the welding spot follows the smoke movement which is of course an expected and wanted behaviour.

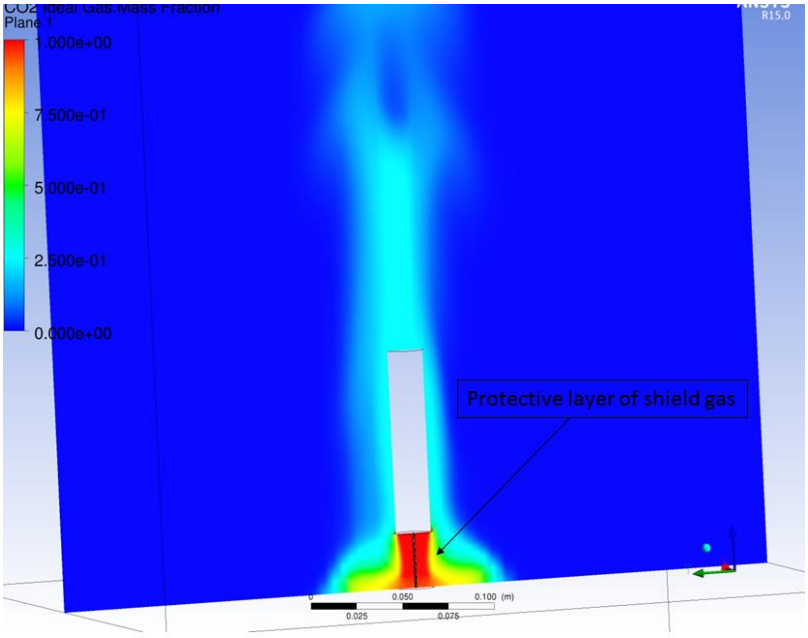

Figure 20, Shield gas mass fraction at centred plane

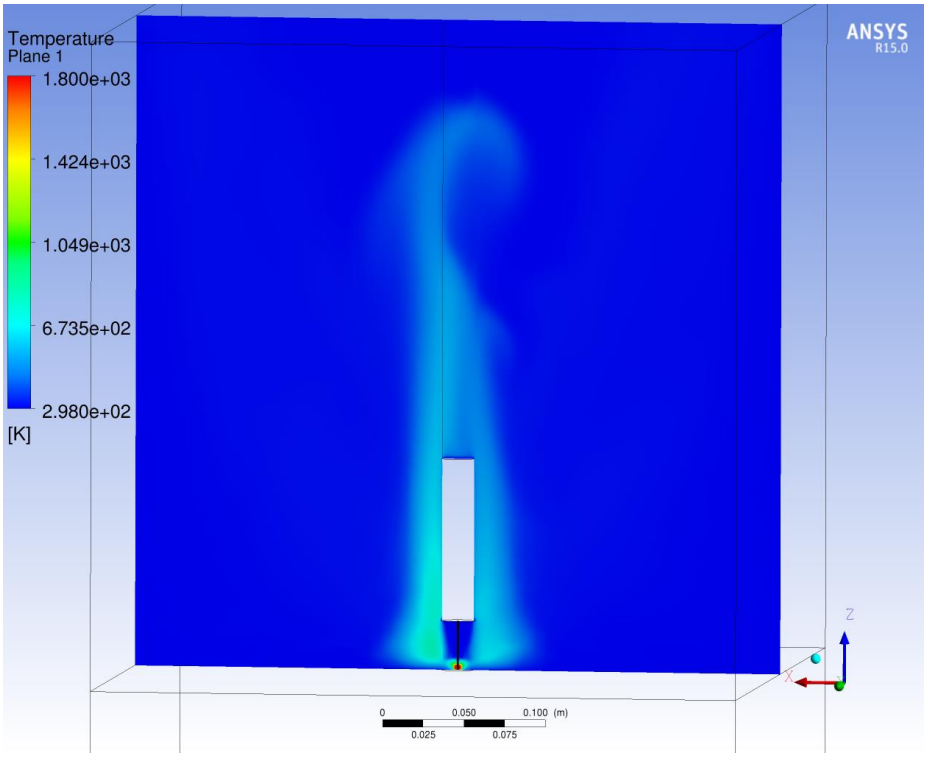

Figure 21, Temperature at mid plane for MIG weld

6.1.4. On-torch Suction

This case is very similar to the standard MIG case but with an on-torch suction device mounted on the handle (see figure 22).The purpose of this device is to suck the fume out without affecting the shield gas flow. More differences is that the domain is cut in half, that the weld is tilted and that the time of simulation is 1.5 s.

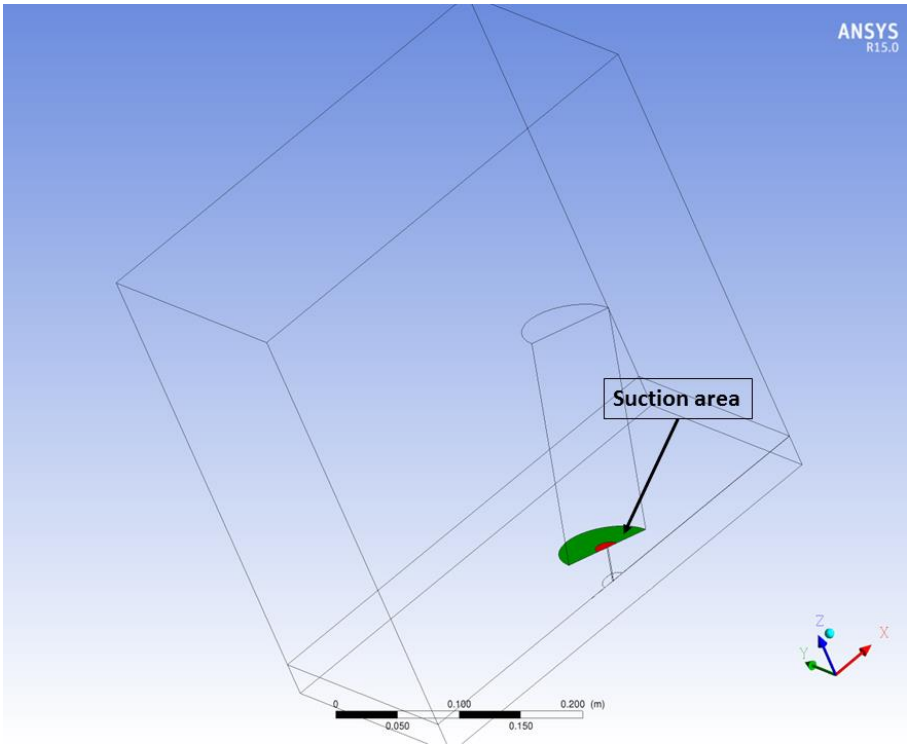

Figure 22, Geometry of 3D on-torch suction

The suction rate has here been set to the unscaled value of 1 m/s with fume release and shield gas rate similar to the MIG case but with area scaled values due to the half geometry.

Iron, which is a part of the fume, can be seen in figure 23 showing the mass fraction. It is clearly visible that all the fume are here drawn into the suction system.

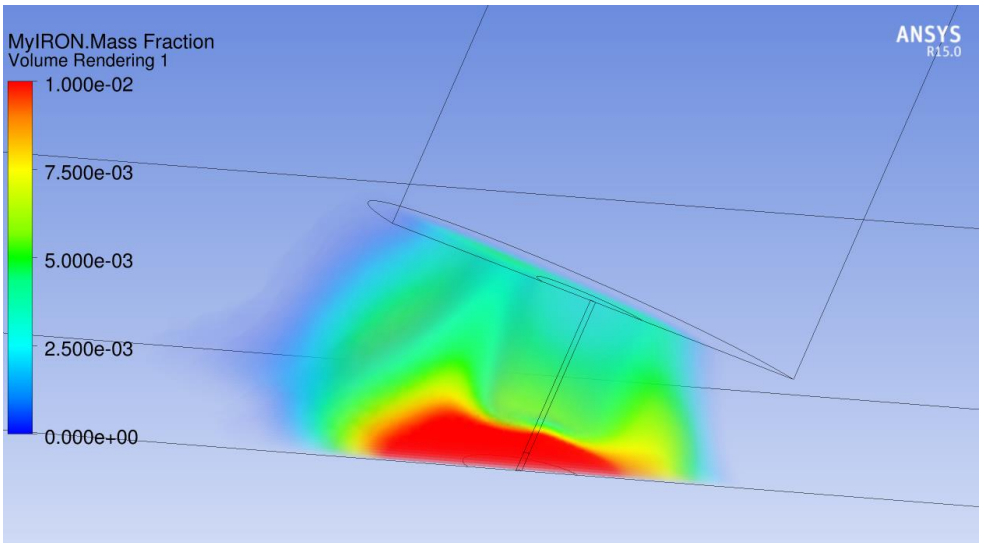

Figure 23, Iron mass fraction of 3D on-torch suction

Another important part of MIG welding is the shield gas which is here pure carbon dioxide. The mass fraction of carbon dioxide is seen in figure 24 and clearly shows that the shield gas is still protecting the melt with this relatively low suction rate. However it is probably not enough since almost no air should be present close to the melt for a good welding result (Sandvik, u.d.). Here parts of the melt only have a mass fraction of around 12.5 %. This phenomenon will be investigated further in the on-torch optimization chapter.

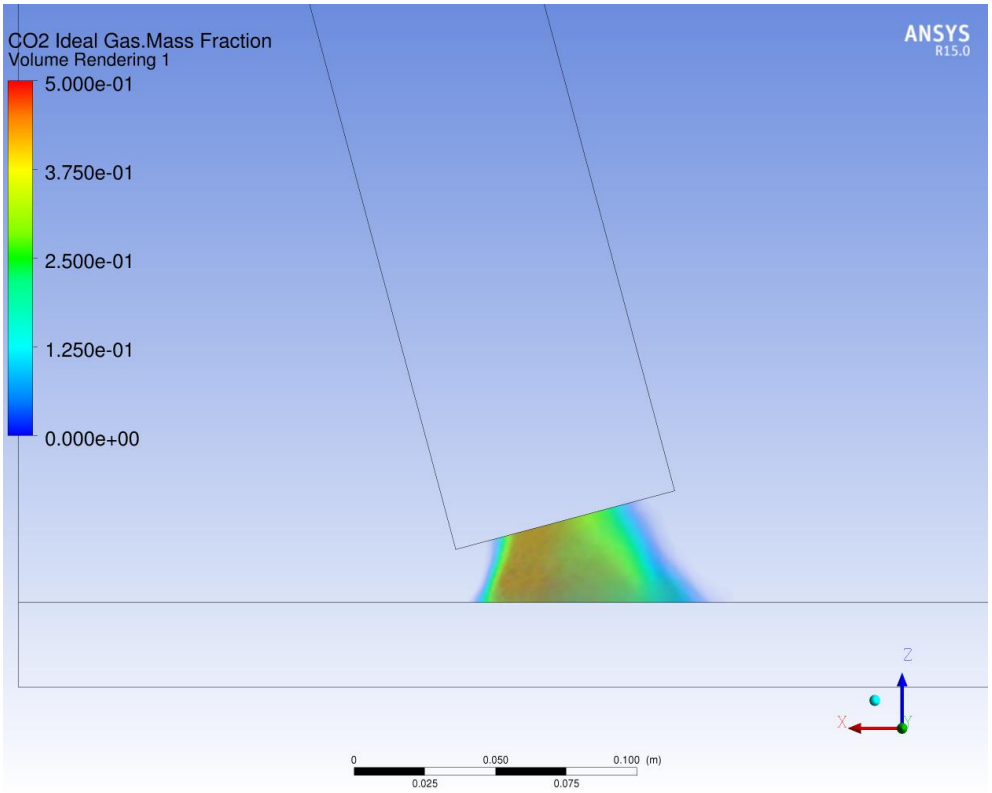

Figure 24, Shield gas mass fraction of 3D on-torch suction

6.1.5. Tilted MIG Weld

There is only one difference between this case and the original three dimensional MIG, namely the fact that the weld is tilted. As shown in the physical phenomena testing, the weld angle is expected to have an impact on the fume flow. In three dimensions it is possible that the behaviour is different than in two dimensions which is why a three dimensional models is needed.

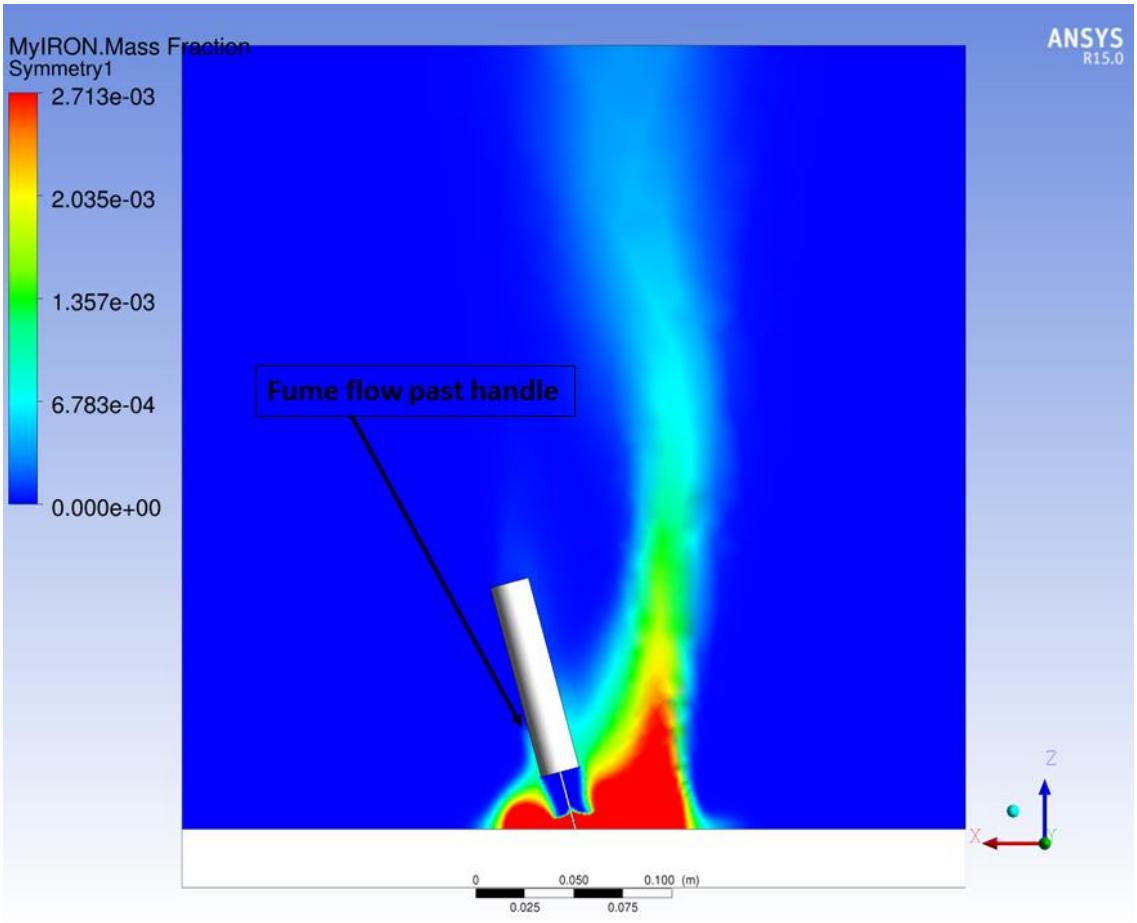

Figure 25, Fume mass fraction, tilted MIG weld

As seen in figure 25 the fume is changing direction from the flow of the shield gas. There is fume flowing past the handle due to this and a close look shows that only a small amount of fume reaches the top of the handle. Results like this can be used to know where to place suction due to the change of fume direction and will be further investigated in the parametric testing chapter.

6.2. TIG (Tungsten Inert Gas)

In this project only a TIG weld without any consumable has been modelled. The TIG method has been discussed earlier in the theory section, but the general difference from the MIG weld is that its electrode is made of tungsten and not consumed during welding. This means that the temperature must not exceed the melting point of tungsten (3695 K) in the electrode. Similarly to the MIG, the TIG uses a shield gas flow from the handle to protect the melt.

6.2.1. Geometry

The geometry is very similar to the MIG case. Fume, shield gas and heat are released from the same surfaces and the only real difference is the dimensions and that the handle has been constructed with a curve shape instead of the earlier straight shape (see figure 26). The change of form on the handle is mainly to show that the model is working although the handle has a different shape since this could occur in reality. Notable is also of course that the domain is split in half with assumed symmetry in order to make the domain smaller and save computing time. Dimensions of the weld, along with electrode and shield gas release can be seen in figure 27.

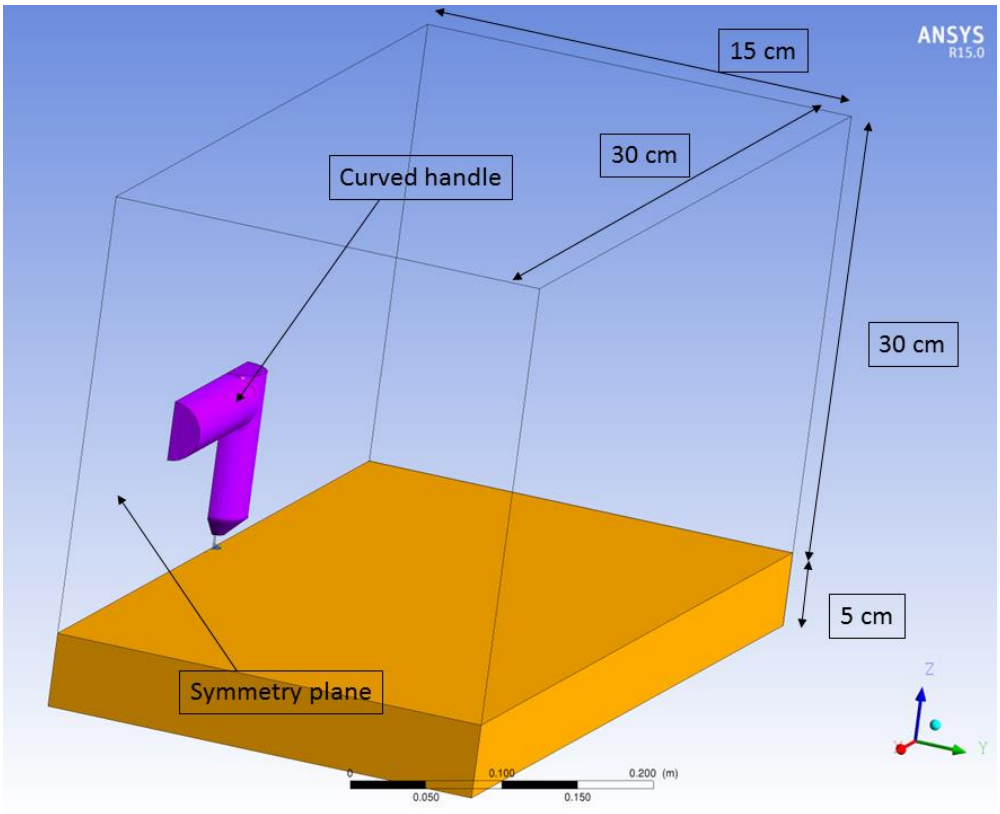

Figure 26, TIG weld geometry

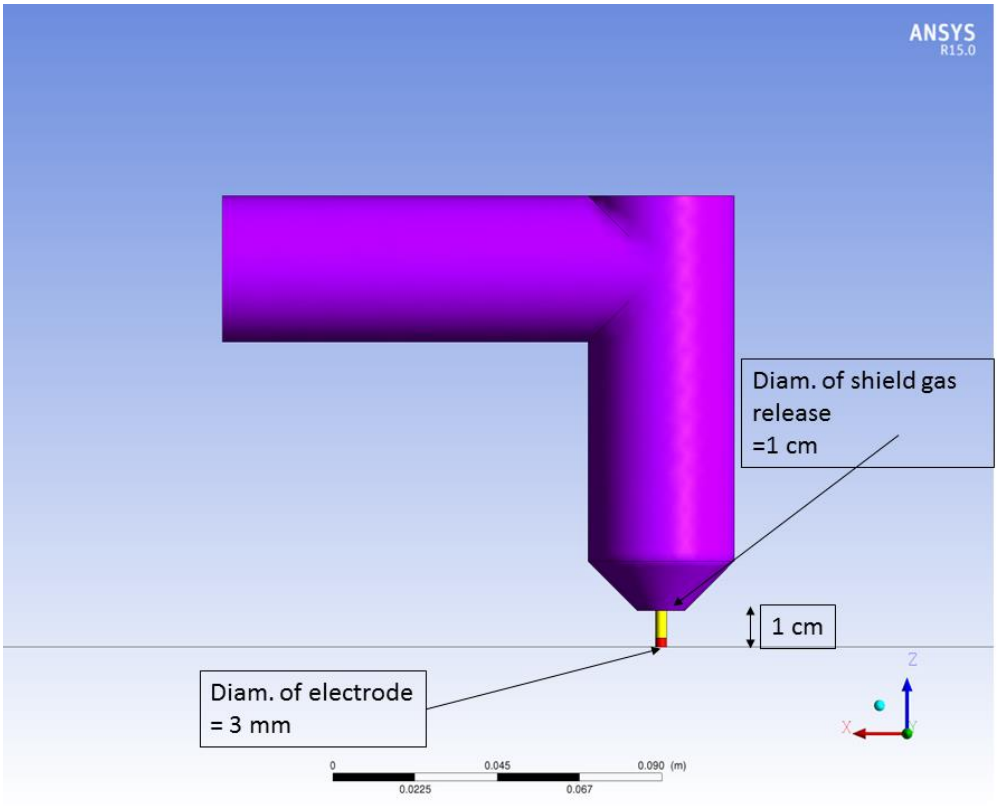

Figure 27, Close up geometry of TIG weld

6.2.2. Setup

Regarding the setup it is quite similar to the MIG, with some differences. The TIG releases a smaller amount of fume with a different composition. This means that it has to be run for a longer period of time, in this case transient for 2 s has been used. It also means that the geometry is allowed to be a little more complex since the velocity will be a bit smaller in the beginning, which is also one reason that a curved handle is used now. Details of fumes (K.Malmqvist, 1980) and shield gas (MIG-welding, u.d.) along with heat release (K.Malmqvist, 1980) can be found in table 4. These values have later been halved due to the surfaces being half of a real structure.

Table 4, Gas and heat release from TIG weld, unscaled values

Current [A]	112
Voltage [V]	12
Heat release [W]	1344
Shield gas, [kg/s] pure Argon	1.67e-4
Chromium [kg/s]	2.96e-9
Manganese [kg/s]	1.85e-8
Iron [kg/s]	8.52e-9

6.2.3. Results

An important aspect of the TIG weld is, as discussed earlier, the fact that it is not wanted for the tungsten electrode to melt. In figure 28 it can be seen from the symmetry plane that the temperature inside or around the electrode does not reach the melting temperature of 3695 K.

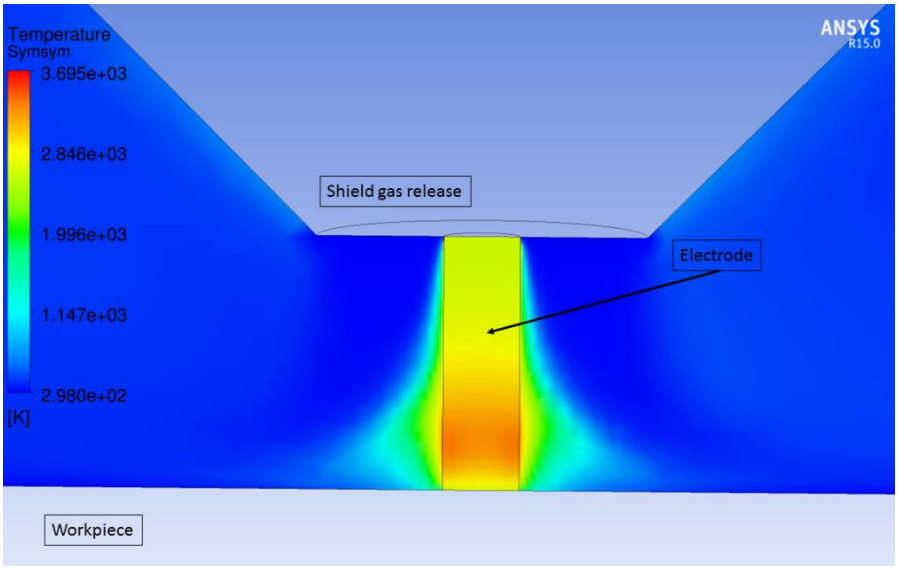

Figure 28, Temperature at electrode where pure red colour is the melting point of tungsten

Figure 29 is showing the fume flow over time at four different moments. As can be seen, the flow is quite similar to the one from the MIG case. However, the low fume release rate makes the shield gas flow pushing the fume further away from the electrode before it is returning in a vortex. The fume is then colliding with the handle which makes part of it move upwards.

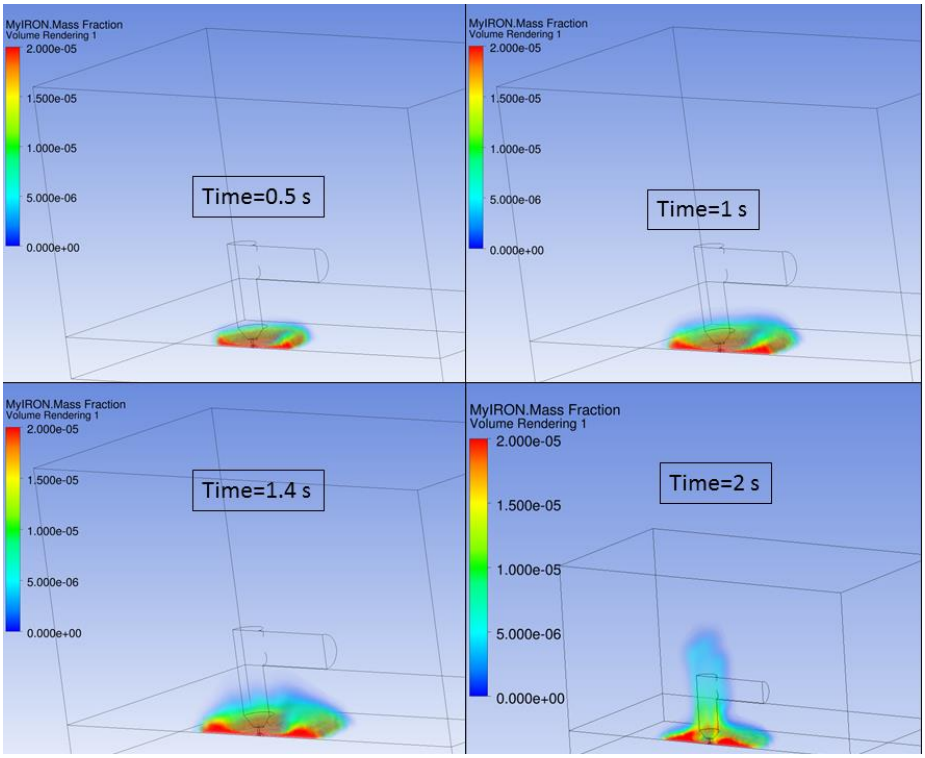

Figure 29, Iron mass fraction for four different moments in time when TIG welding

From the vectors, showing velocity direction of the flow, the vortices can be seen clearly in figure 30. Here it is also noted that the fume rises higher on one side of the weld compared to the other. Since a curved handle is used, it creates a delay of the fume flow on the curved side. The reason for this is that the flow direction close to the handle curve is partly against the fume flow direction and therefore slowing down the fume rise. This can easily be seen by the directions of vectors close to this part which is marked with red arrows in the figure 30. Conclusions that can be made from this is that the geometry of the handle can affect the fume flow to a great extent.

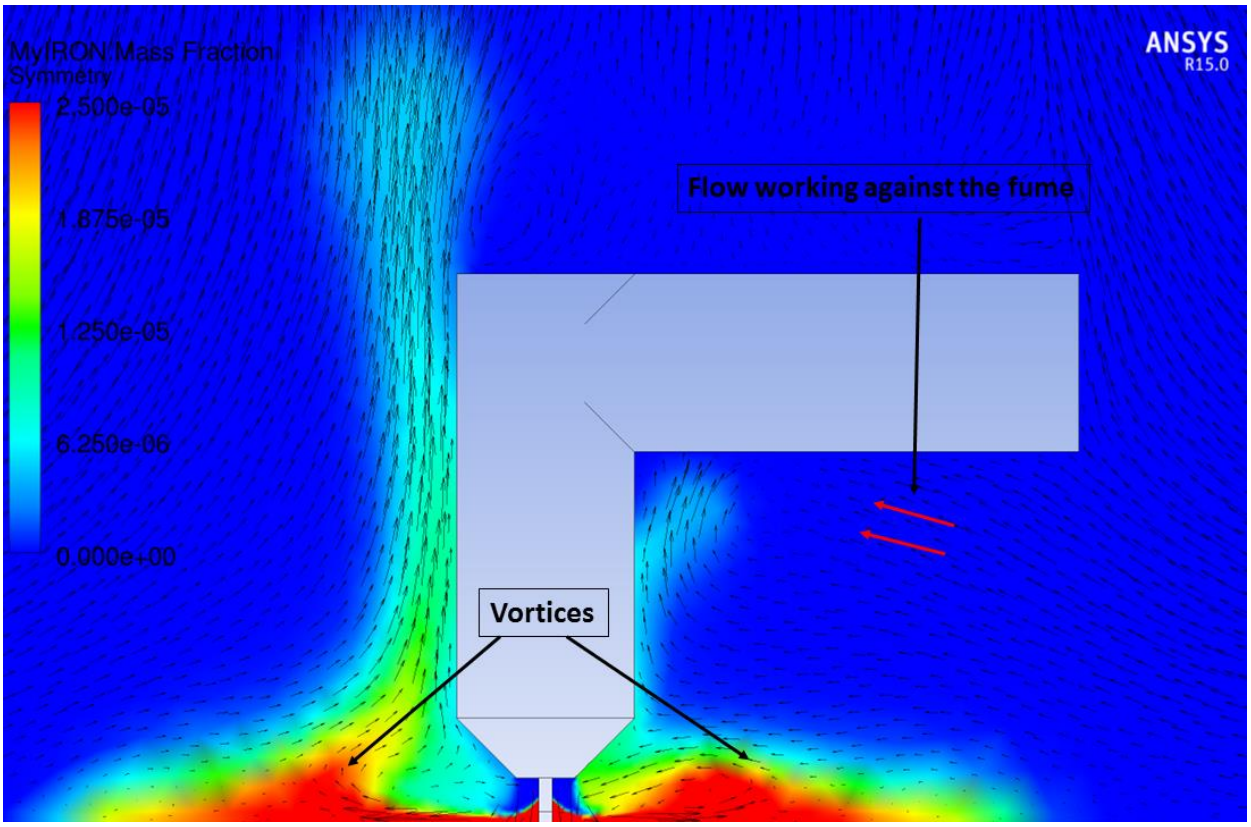

Figure 30, Vectors showing flow direction in the fluid domain on the symmetry plane where iron mass fraction is shown

That the fume is warm like it was in the MIG case and would be in a real case is clearly shown in figure 31. Here it can be seen, in comparison with figure 30, that the higher temperature follows the flow of fumes very closely. A small cold part is present around the electrode as well. This is caused by the cold shield gas flow and also means that there is at least some shield gas present to protect the molten part.

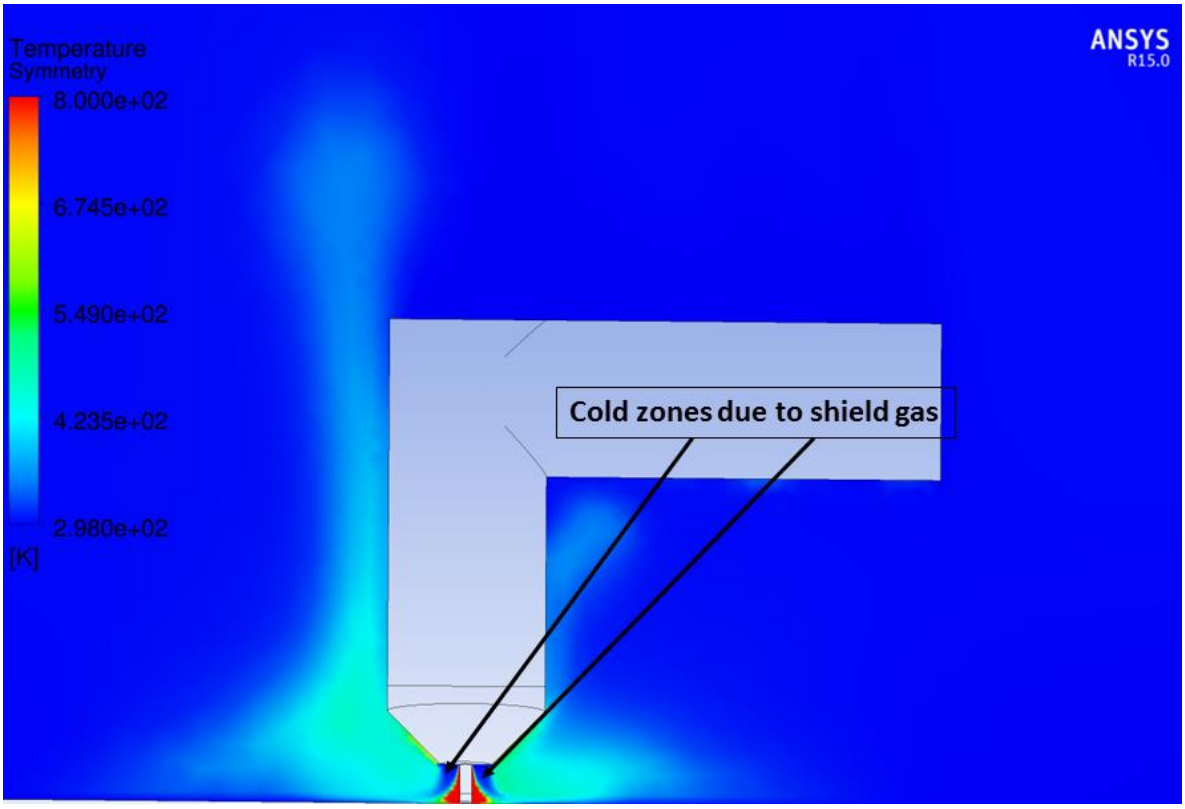

Figure 31, TIG welding temperature at symmetry plane

6.3. SMA (Shielded Metal Arc)

Regarding the shielded metal arc welding or "stick welding", it differs a little from the previous two welding methods. Details of the method can be seen in the theory section but it will here be very briefly summarized. The electrode is consumed but there is no shield gas flow from around the handle. Instead the gas used for shielding comes from melting the coating around the electrode.

6.3.1. Geometry

Similarly to the other two welding methods, the SMA is built up with an electrode and a handle. The electrode is however considerably longer than for the other cases since it is consumed and has to be replaced after a while. In this project, the electrode has however been assumed to be of constant length and moving as the electrode in the MIG case to simulate the fact that new cold material is coming closer to the molten part. Apart from the electrode diameter (3.25 mm), dimensions and details can be seen in figure 32 where it also can be seen that the shield gas release is situated at the same warm part as where the heat is released. Regarding the fume it is once again released from the fume release surface (see figure 32). The domain is, as in the TIG case, split in half to provide a faster model with the assumption of symmetry.

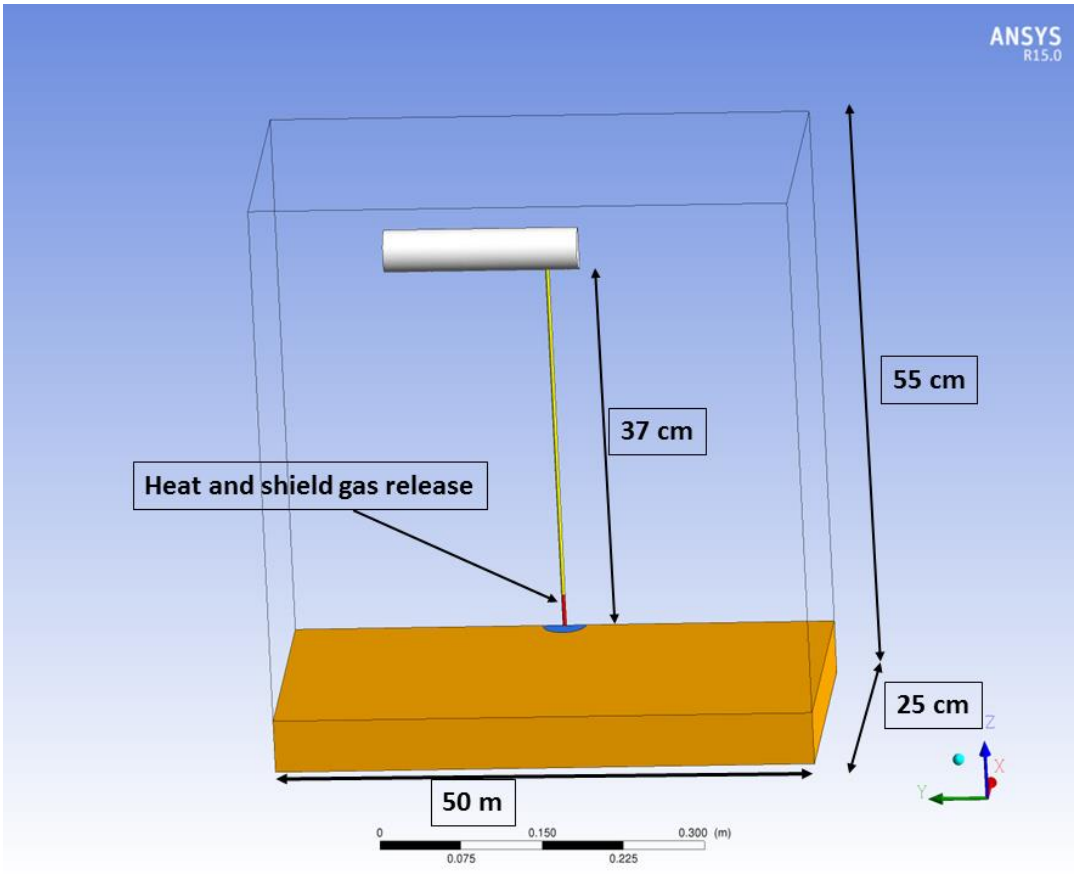

Figure 32, Geometry of SMA weld

6.3.2. Setup

This is a transient run for about 3 s and as mentioned above, all releases come from the same region around the bottom of the electrode. This means that all other solid parts are handled as steady fluid-solid interfaces. The electrode has a downwards velocity of 1.4e-6 m/s (ESAB, u.d.) because it is consumed during welding. As base the electrode is an OK 48.00 but with the assumption that it is without coating in the solid. This is an acceptable assumption since previous tests have shown that the thermal conductivity of the solid did not affect the end result too much. The fume and gas release has however taken the coating into account and the composition can be seen in table 5, where the values are later scaled, with the area as base, before usage. Notable is that the release has been divided into fume and shield gas. The fume consists of manganese, iron, oxygen and titanium while the shield gas consists of calcium, fluorine and potassium. However they are generally the same gas for this case. In table 5 the heat release can also be seen as calculated from the current and voltage.

Table 5, fume and shield gas composition along with heat release of SMA welding (K.Malmqvist, 1980), unscaled values

Shield gas	
Calcium [kg/s]	5.4264e-7
Fluorine [kg/s]	8.6744e-7
Potassium [kg/s]	8.596e-7
Fume	
Iron [kg/s]	1.279e-6
Manganese [kg/s]	2.548e-7
Oxygen [kg/s]	1.76e-6
Titanium [kg/s]	2.352e-8
Heat release	
Current [A]	110
Voltage [V]	23
Heat release [W]	2530

6.3.3. Results

In figure 33 it can be seen that the vortices in the MIG and TIG welding are not present. This is due to the lack of a shield gas flow that pushes the fume outwards. Instead, the gases are released and heated which makes them drop in density and rise straight away.

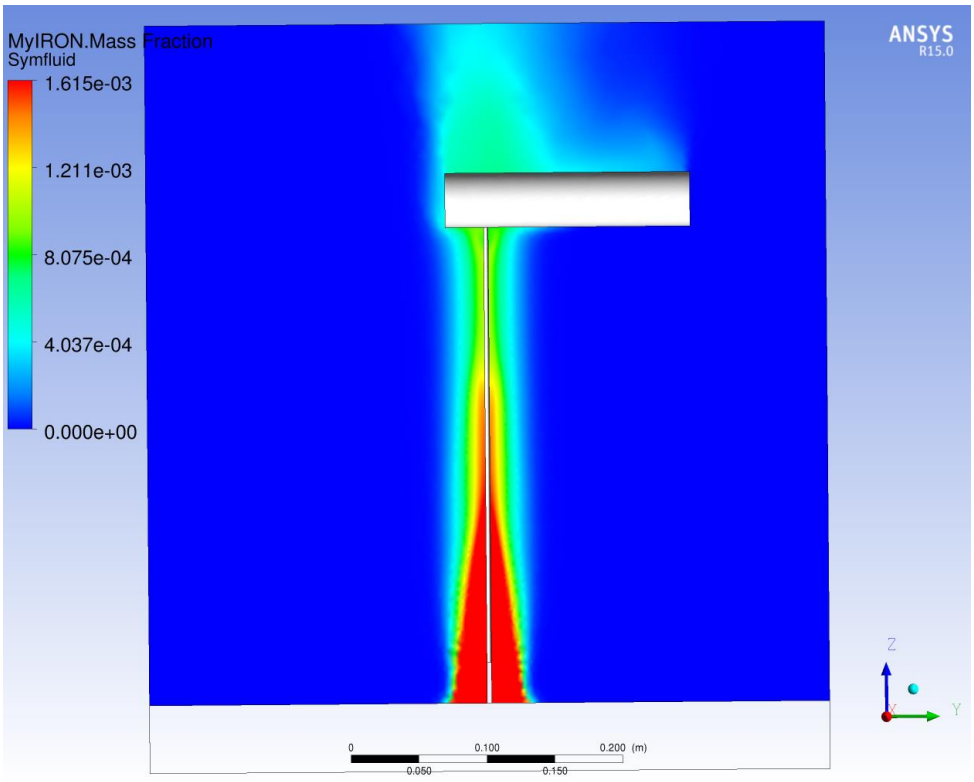

Figure 33, Iron mass fraction at symmetry plane

Because of the quick rise of gases, the SMA weld reaches a state where there are no essential new features happening, quite fast. This can be seen in figure 34 where the oxygen flow looks the same for 1.5 s in comparison with 3 s. It can then be concluded that the SMA do not need a long time to run and it is therefore suitable to use this model for simulations with a larger fluid domain.

Since there is not an actual shield gas in this case it can be seen in figure 33 that there are fumes shielding the molten part and lying as a protective layer around the electrode.

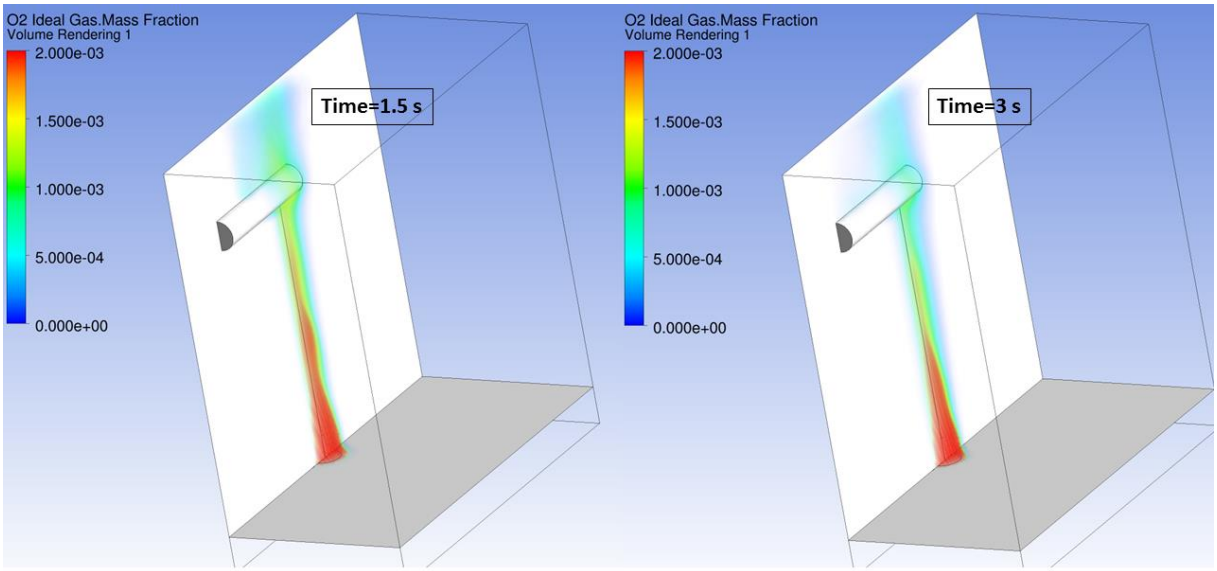

Figure 34, Mass fraction of oxygen over time

6.4. Discussion

It can be said that the fume flows in the three dimensional models behave much as anticipated and are close to a real fume release from welding. Along with this, the shield gas lies as a protective layer over the molten part in all these cases which is also similar to reality. This shows that the models are accurate and reliable. However, there are a few problems. It is quite time consuming to run a transient simulation in three dimensions with the high temperature that is created from welding. It is not possible to create a steady state model since this often leads to convergence problems. In this project, efforts to make a quicker model have been made through using a smaller domain and using fewer meshing cells at unimportant regions. A strategy to be able to use a larger domain could be to set the values from a smaller domain as boundary conditions in a larger. This would mean that it is not needed to calculate the smaller domain containing the weld after a period of time. It would then give possibilities to run longer simulations and test more different values.

Regarding the movement of fumes they all rise along the electrode or handle which would mean that a suction could be placed at any altitude along the electrode and still be able to reach the fume. However, a tilted weld is expected to change this fact. Suction will be further discussed and tested later in this project.

7. Parametric Testing

It is of great interest to perform tests in order to see the parameters that are correlated to the fume movement. For example it could lead to better protection of the welder since the fume could be reduced in certain areas. It could also lead to better knowledge of where suction should be placed. Software used for this performance is ANSYS CFX, controlled with the use of modeFRONTIER.

7.1. Geometry

Used in this case is a two dimensional tilted MIG weld (see figure 35) with zones created at the outer boundaries of the fluid domain. These zones are created in order to detect where the fume fraction is high. The dimensions of the fluid domain are 40 cm in width and 30 cm in height. Details of the geometry can be seen in figure 35.

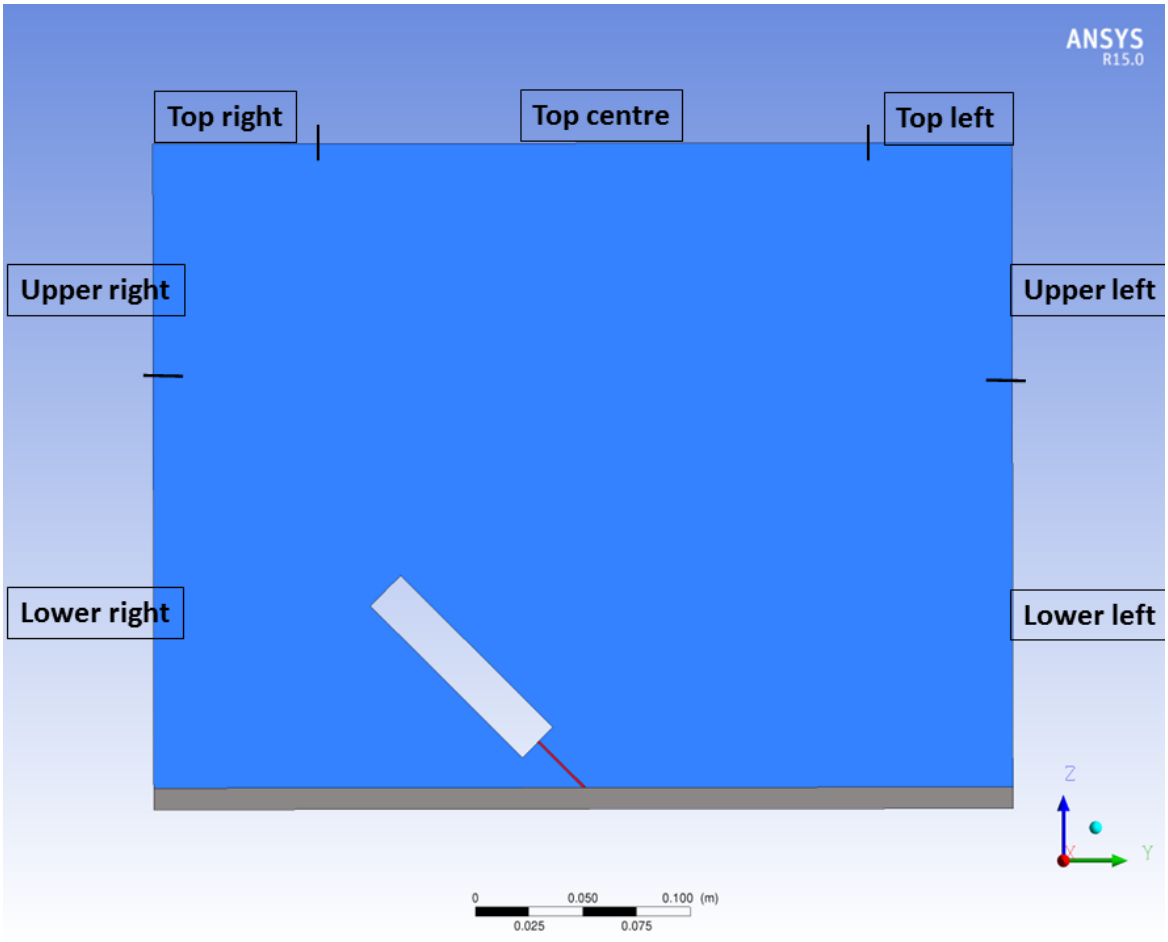

Figure 35, Geometry of parameter testing case. The different control zones are especially marked

7.2. Setup

The setup for the ANSYS CFX project is similar to the three dimensional MIG case but with scaled values. Electrode and workpiece materials are set to a standard steel used in ANSYS CFX (ANSYS CFX, u.d.). The flow of gases and heat comes from the same surfaces as described in the physical phenomena testing section and table 6 shows the unscaled flow values in detail. For all different designs, a transient run of one second has been used. The procedure of correlations used is the Pearson approach.

Table 6, Gas flow and heat release values for parameter testing case (R.F.Heile, 1975)

Current [A]	200
Voltage [V]	30
Heat [W]	6000
Shield gas, 100 % CO2 [kg/s]	7.85e-4
Silicon [kg/s]	1.2167e-6
Iron [kg/s]	2.1e-6
Manganese [kg/s]	3.1667e-7
Oxygen [kg/s]	1.0167e-6

7.3. Parameters Varied

The strategy for choosing parameters to vary is based on the physical phenomena testing. From this it could be seen that changing the material in the electrode did not affect the result too much. It is also assumed that the composition of the fume and the fume release rate will not have a large effect on the fume movement itself. However, some parameters have shown to be of interest. These are the weld angle, the heat release and the shield gas rate. The weld angle affect the flow direction of the shield gas and will therefore push the fume towards a certain direction. Heat release affects the fume movement in the sense that the density becomes lower which will increase the rate of fume rising due to buoyancy effects. Finally the shield gas is, as mentioned before, pushing the fume outwards, in many cases creating vortices. Then the velocity of this will of course affect how far out the fume is pushed and therefore affect the movement. Figure 36 shows the parameters varied, where it is notable that a weld angle of 90 degrees answer to a totally vertical electrode.

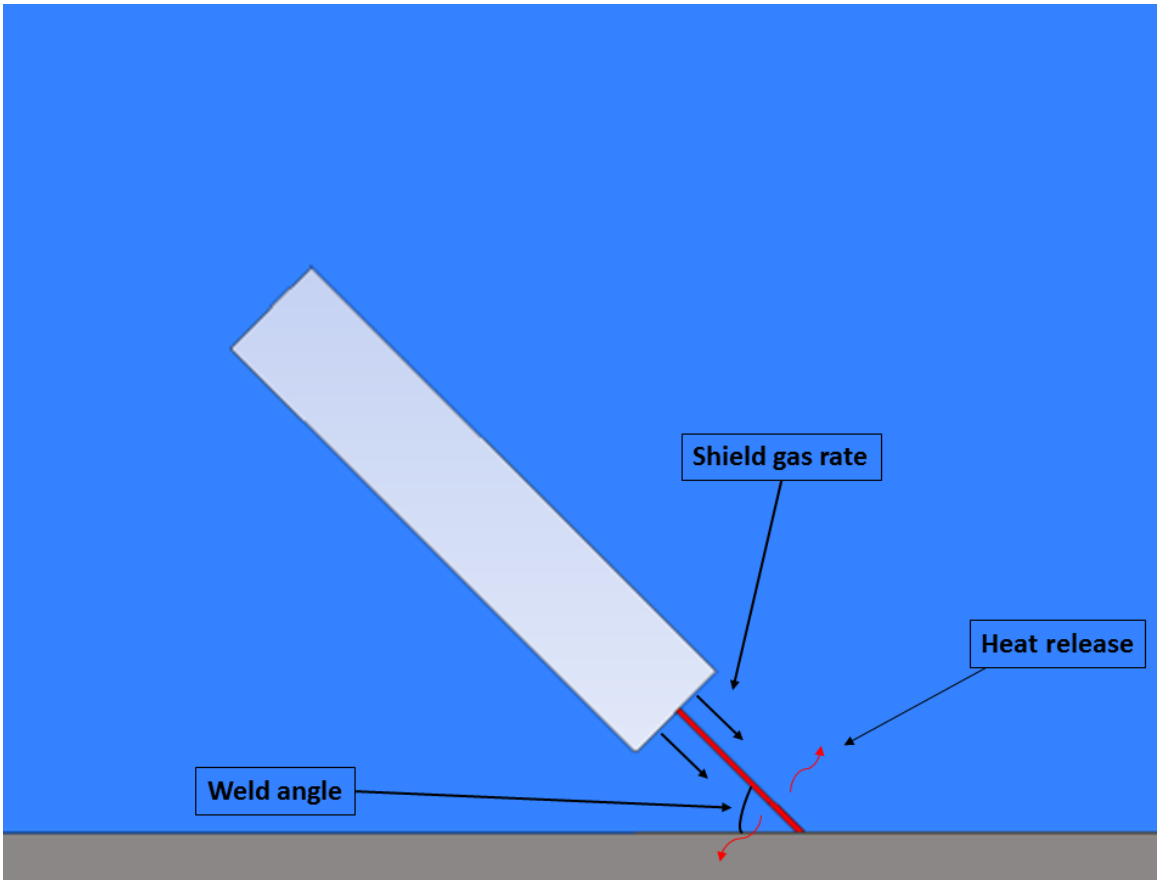

Figure 36, Parameters varied

7.4. Design of Experiment (DOE)

The DOE contains the points chosen for testing. It should contain different combinations of all values in order to test as many options as possible. For this case the Uniform Latin Hypercube method has been used. Twelve different points were considered with the assumption that the variable parameters all have a quadratic behaviour. In order to define a quadratic line, at least three points are needed and to define a quadratic surface with three variables, at least ten points are needed (Wolfram Mathworld, u.d.). With a margin for safety set, twelve points were decided. The entire DOE can be seen in table 8 along with the parameter range in table 7. These values are later scaled with the area as base since it is a two dimensional model. The range of the parameters has been chosen from constraints such as the fact that the weld cannot be too tilted since then it collides with the workpiece. The other two parameters are just set within reasonable values, from electricity when it comes to the heat release rate. Regarding the shield gas rate a high upper limit has been set for curiosity reasons mainly and since the model is known to work even with these high values. This would not be possible with the heat release rate due to convergence problems.

Table 7, Parametric values interval

Parameter range	**Lower value**	**Upper value**
Shield gas rate [kg/s]	3.926e-5	1.963e-2
Heat release rate [W]	1587	15870
Weld angle [degrees]	40	90

Table 8, Design of experiment

Design ID	Heat release [W]	Shield gas rate [kg/s]	Weld angle [degrees]
0	7372	0.004	69.01
1	7935	0.004	69.01
2	5521	0.006	83.36
3	12531	0.013	87.27
4	9913	0.016	43.67
5	10486	0.001	58.11
6	1892	0.006	52.57
7	4989	0.015	80.81
8	15297	0.008	71.77
9	11651	0.018	63.07
10	3281	0.011	46.94
11	8485	0.010	75.65

7.5. Results

First of all the correlation matrix, seen in figure 37, will be presented. As can be seen, the weld angle is correlated to the direction of the fume movement. A large angle (more vertical weld) means that more fume is reaching the so-called left side which is expected since the fume is often moving along the handle. Smaller weld angles means more fume at the right side which probably comes from the same reason that the fume is moving along the handle and then reaching upwards. With a tilted handle it is therefore reaching further to the right side.

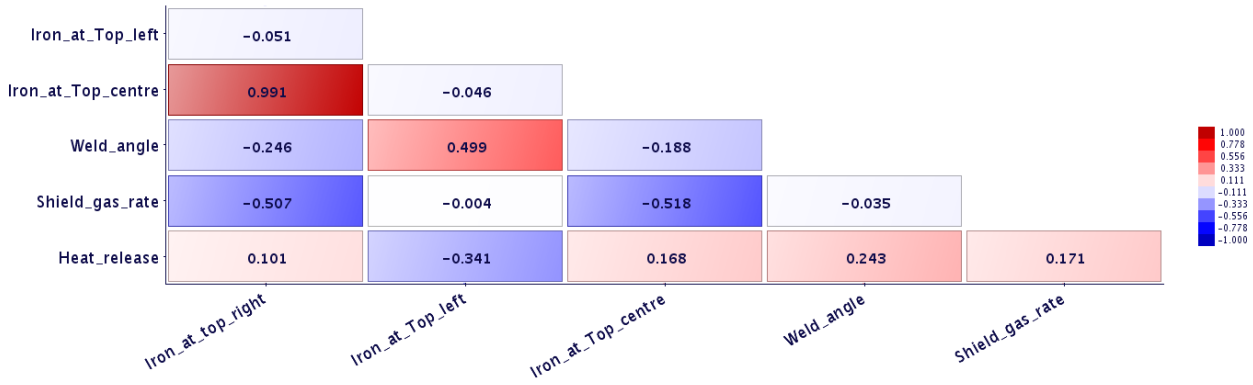

Figure 37, Correlation matrix, parametric testing

More results from the correlation matrix (figure 37) is that a higher shield gas rate means lower amount of fume at the top. This comes from the fact that the shield gas flow is pushing the fume down and therefore it does not reach the top area. Noted is also that the heat release is not affecting the fume flow to any large extent here. However, more heat means a little more fume at the top of the domain which is expected since more heat means lower density for the fume.

One problem with this correlation matrix is seen in the correlation between the weld angle and the heat release. This correlation is positive and shows that a higher heat release would give a slightly higher weld angle. However, this is not the case since both of these values are input parameters and are not correlated at all. The reason for this false correlation is merely the method used where all parameters are correlated and it is important to be observant on these events.

A design that has a much tilted weld (small weld angle), but yet low value on heat release and a medium value of shield gas rate, is design 6. The fume mass fraction from this design can be seen in figure 38 where it is noted that the shield gas flow creates a number of vortices leading the fume back against the handle. The fume then hits the handle and turns upwards and most of it finally reaches the top-centre region.

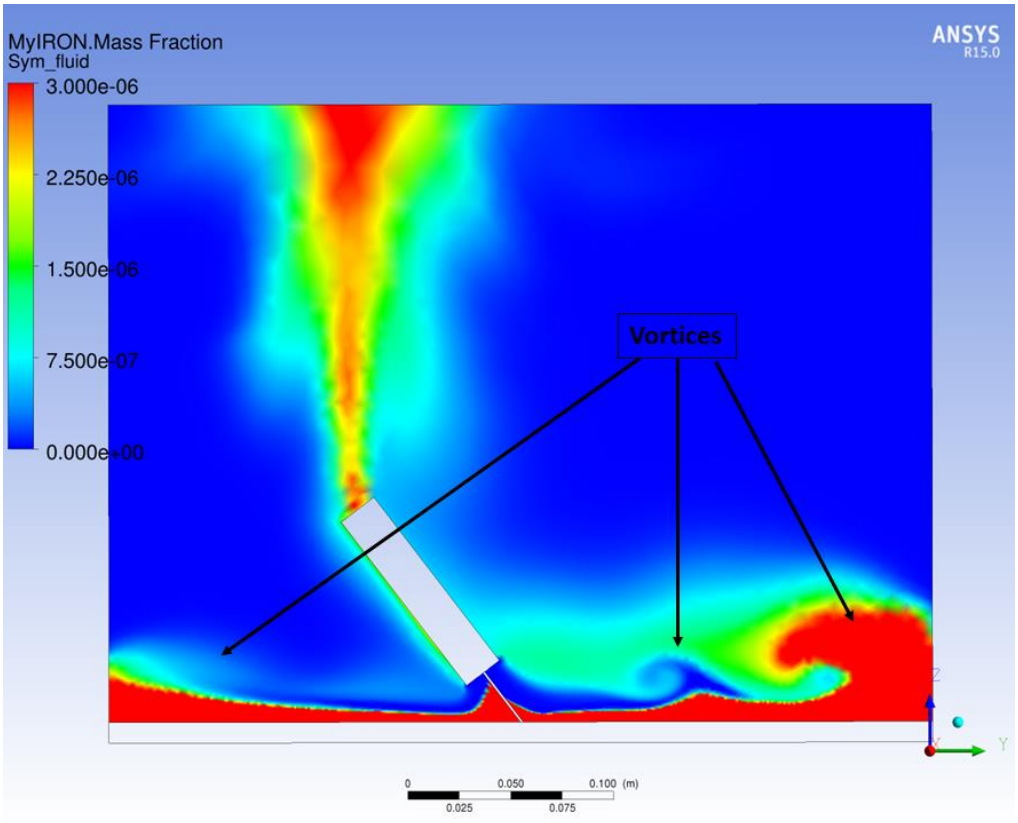

Figure 38, Fume mass fraction, design 6

Design 3 has a weld angle of ca 87 degrees which means that it is almost not tilted at all. Fume mass fraction of this case can be seen in figure 39. The difference for this design in comparison with design 6 is that the fume is more centred at the top of the domain due to the weld angle. Fume is still, through vortices, led back against the handle and heading upwards after collision.

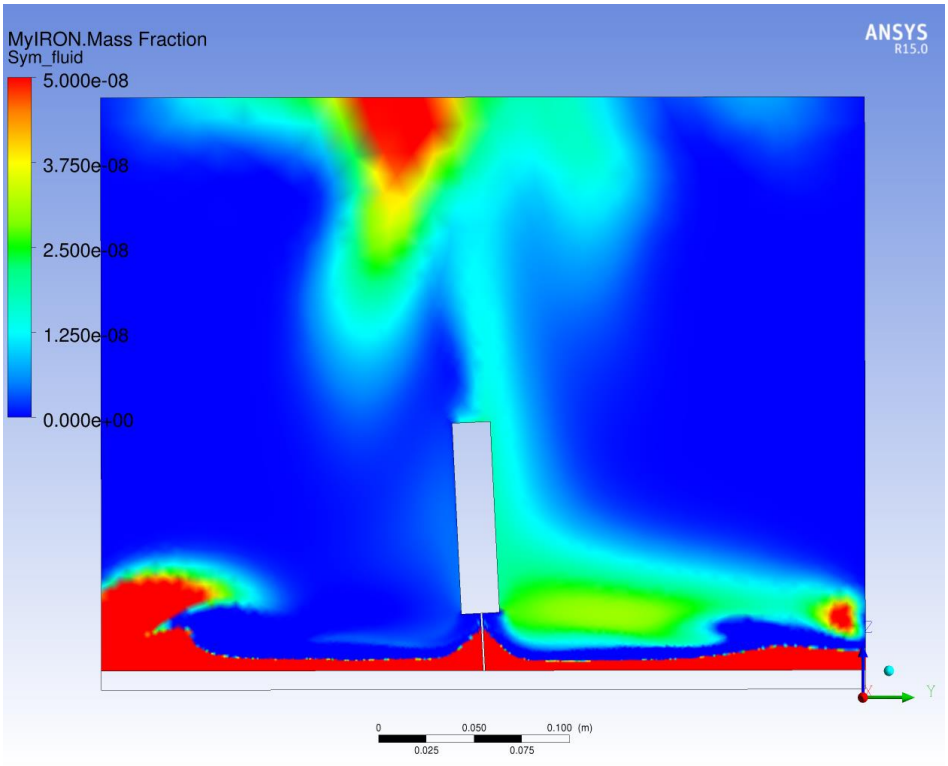

Figure 39, Fume mass fraction (low value range), design 3

7.6. Discussion and Conclusion

Regarding the weld angle it seems, from some of the results, as if it does not affect the fume flow too much. It is still flowing back to the handle and then heading upwards and the only real effect seems to be that the handle reaches further to the side in the tilted case. However this is due to the fact that these simulations are run in two dimensions. For three dimensions the fumes are allowed to pass around the handle which would probably be the case here. Therefore it can be concluded that tests in three dimensions would have to be carried out before any totally reliable results can be achieved for the weld angle. However, it can be noted from this case that the weld angle indeed does matter and enhances the creation of vortices in the domain.

More conclusions is that the heat release does not affect the fume movement too much, at least not in this parameter range. The important matter is the direction of the fume and the heat is mostly affecting how quick the fume rises. Heat is easy to regulate for the welder since it is based on the electricity. However, there are many more aspects of the heat than just fume movement, such as quality of the welding. These aspects must also be taken into account when altering parameters.

Regarding the shield gas rate, it affects the direction of the fume flow both through pushing the fume down, creating vortices and through pushing the fume outwards from the electrode. A strong shield gas flow could possibly be used for keeping the fume from rising which could aid placement of suction. However, shield gas is expensive and the aim is always to use as little as possible.

Finally it can be said that more parameters are expected to have impact (although to a smaller extent than the ones tested here) on the flow, such as material composition of the fume and movement of the air from the surroundings. It would also be valuable to test more designs and a wider range of parameter values. Here some designs with for example small weld angle could possibly show the wrong result since it is possible that there is also a very high shield gas rate for that design. Therefore more designs could be used here to get an even more accurate result.

8. On-torch Optimization

Optimization is useful for many types of areas in order to see the most beneficial values of certain parameters. In many cases a trade-off between certain parameters must be made. For example in the automotive industry where lower environmental emissions could mean lower performance. This is also the expected case for welding fume release. The example here is on-torch suction where a suction device is placed on the outside of the weld handle. Suction such as this is aiming to collect as much fumes as possible without restraining the shield gas from protecting the melt. A trade-off is expected between these two parameters.

8.1. Geometry

The geometry is similar to the one in the parametric testing case but with an entirely vertical weld geometry. As can be seen in figure 40 there is also a wider handle since an on-torch suction device is mounted on it. Apart from this, dimensions of the geometry are similar to the parameter testing case apart from the electrode length.

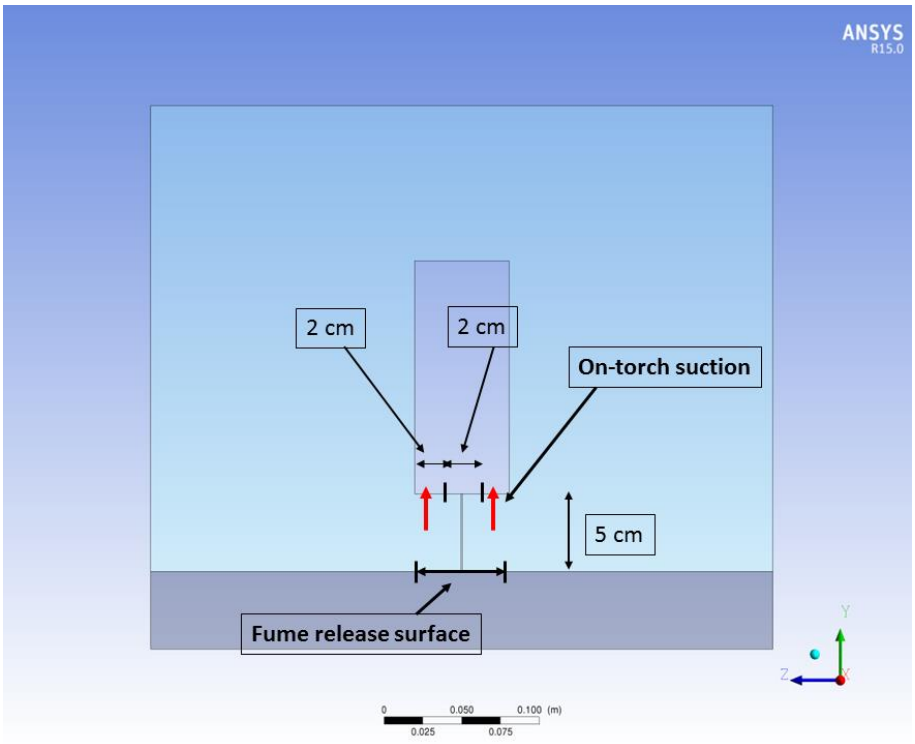

Figure 40, Geometry with on-torch suction

8.2. Setup

The software used for the optimization is ANSYS CFX where modeFRONTIER controls the simulations. Regarding the setup in ANSYS CFX it is, like the geometry, very similar to the parametric testing case. The value for heat release is scaled with respect to area from 6000 W and the fume release is similar to the three dimensional MIG case (see table 3). Simulations are run transient for 0.5 seconds since this is expected to suffice due to the small distance between fume release and suction.

In modeFRONTIER the targets are set to maximize fume into the area of suction (see figure 40), to maximize the shield gas at the molten part of the workpiece (fume release area in figure 40) and finally to minimize the rate of shield gas. The final target is mainly for reducing costs while the other two targets have been discussed earlier.

8.3. Parameters Varied

Chosen parameters to be varied are here the shield gas rate and the suction rate which can be seen in table 9. The reason for this is that the aim of this simulation is to find an optimum between the shield gas protection and the fume suction. A higher shield gas rate will mean a better protection layer around the molten part. However fume suction will be more difficult since the shield gas flow is forcing the fume away. On the other hand, the suction rate will increase fume suction with a higher value but also restrain the shield gas from moving downwards to the melt. This will create a trade-off between the two parameters and is the target to be evaluated here. Method for correlating the parameters has been Pearson correlation.

Table 9, Parameter values on-torch suction

Parameter	**Minimal value**	**Maximum value**
Shield gas rate [kg/s]	1.0e-6	5.0e-4
Suction rate [m/s]	1.0	10.0

8.4. Optimization Method

To start with, a DOE consisting of 24 different designs will be created. The designs can be seen in table 10 in the appendix and the use of these designs is to get a view of the behaviour of the different outputs. Results from this run will then be used to build a response surface. A response surface is a surface that approximates the behaviour of the results into a mathematical function.

The response surface is then evaluated with verification points taken randomly from the DOE. If the response surface is not regarded as suitable, a simulation with new designs is performed. These designs are chosen with a number of techniques. One technique is to fill empty areas on the response surface with new designs. These areas are found through looking for the largest smallest distance between two of the points. This is called incremental space filler in modeFRONTIER. Here, nine points are chosen with this method (see table 11 in the appendix).

Another technique is to find areas on the response surface with high gradients. The reason that these areas are interesting is since high gradients mean zones with a changing behaviour. This could both mean that this area is important and that there are too few points there. Too few points would lead to an incorrect response surface. This filling method called Lipschitz sampling is used for choosing the last five points in this optimization procedure (see table 12 in the appendix).

A new response surface is then made and once again checked against verification points and, if the result is satisfying, used for creation of 4000 new designs. The method for this is ULH for the first 40 designs and MOGA-II for the remaining amount. These designs are only based on the response surface. Optimal points will then be found through the use of a Pareto front. The Pareto front is showing where the trade-off between the different outputs is the best. It could be just a single point or many points, it depends on the response surface. A single point means that this is the optimum since if the values are changed in any direction, a worse trade-off point will be achieved.

8.5. Results

An example of a case that does not catch all fume is design 37. The mass fraction of fume can be seen in figure 41 were it is noted that there is “escaped” fume present above the suction.

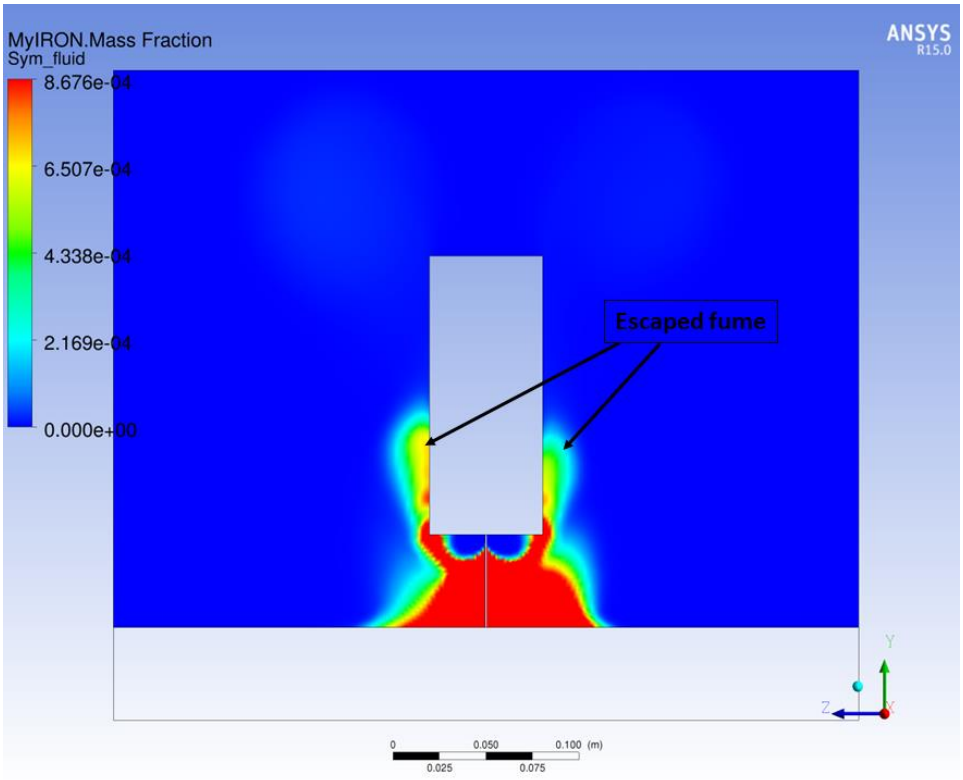

Figure 41, Iron mass fraction of design 37

The shield gas flow for design 37 can be seen in figure 42 where it is noted that vortices appear above the handle. Escaped fume will probably also enter into these vortices which means that the fume will be trapped here. In this area it could then be possible to place another suction and catch the fume here. The protection from the shield gas is however not satisfying since the mass fraction of shield gas close to the melt is only around 12 %.

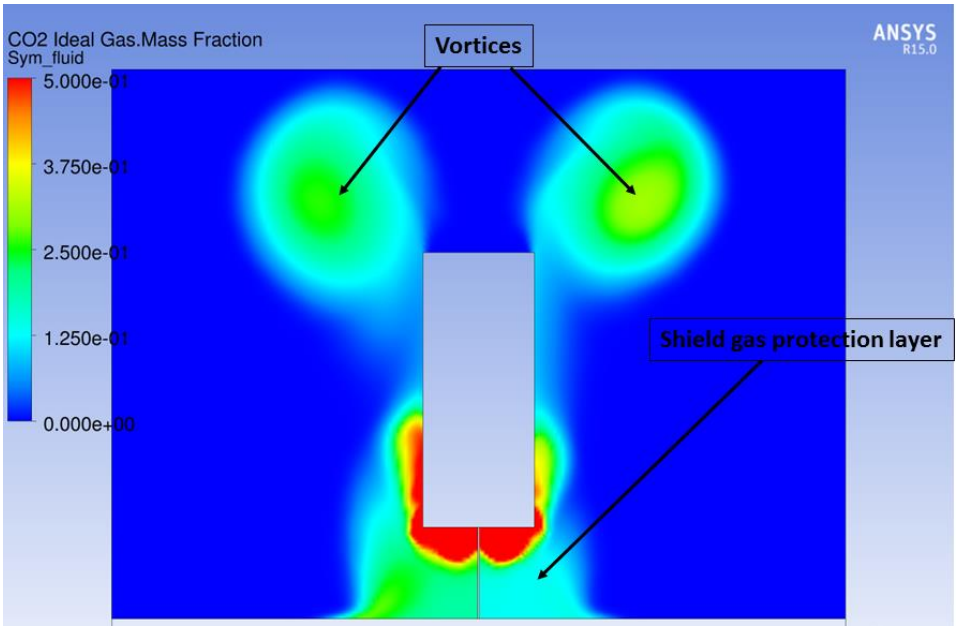

Figure 42, Shield gas mass fraction, design 37

Regarding cases with very good melt protection from shield gas, design 27 has been evaluated. In figure 43 it is seen that the shield gas covers the melt with a mass fraction of around 100 %. It is also noted that almost too much shield gas is present with the entire workpiece covered. This is not wanted since one of the targets is to minimize the shield gas rate.

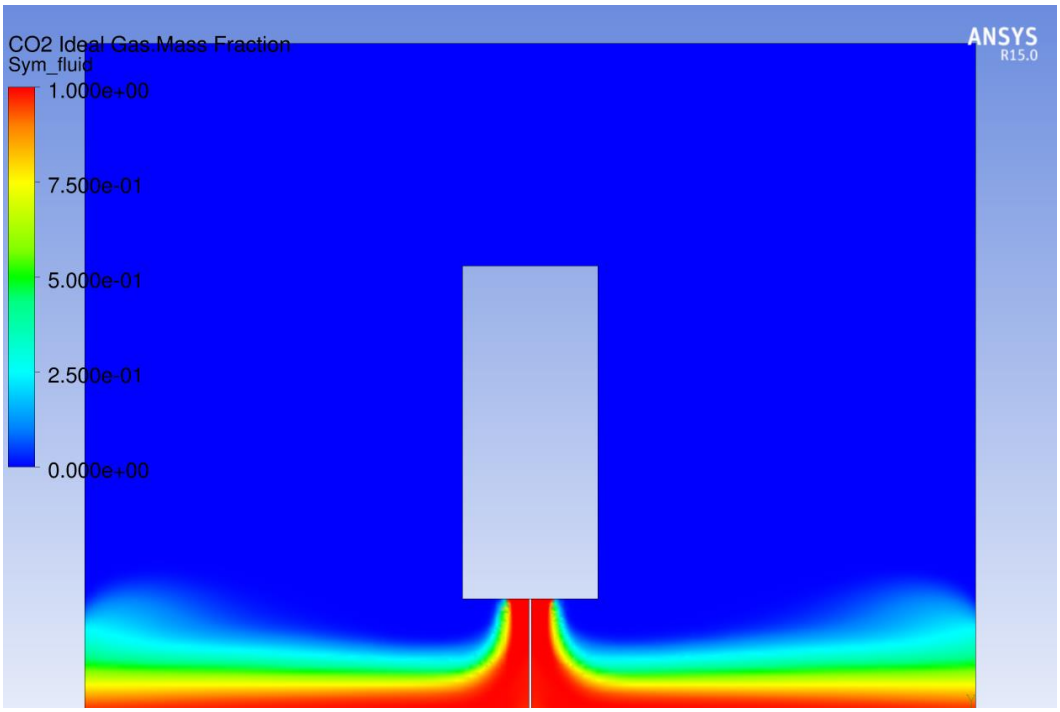

Figure 43, Shield gas mass fraction, design 27

A very good design for fume capturing is design 32, shown in figure 44. In this figure it is seen that no fume escapes the suction which is the wanted result for protection of the welder. However the shield gas, shown in figure 45, is not present at the melt to any large degree with only around 0.0075 % mass fraction of shield gas at the boundary of the melt.

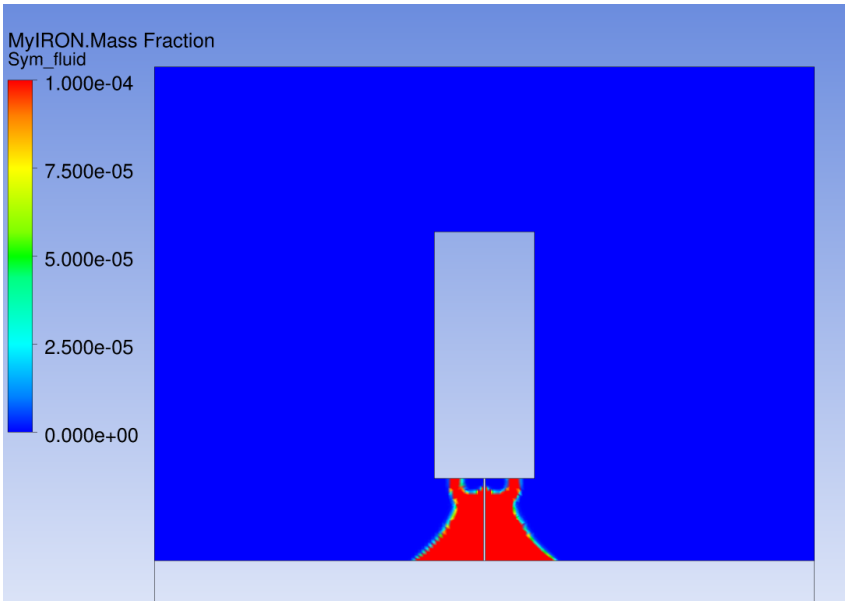

Figure 44, Iron mass fraction, design 32

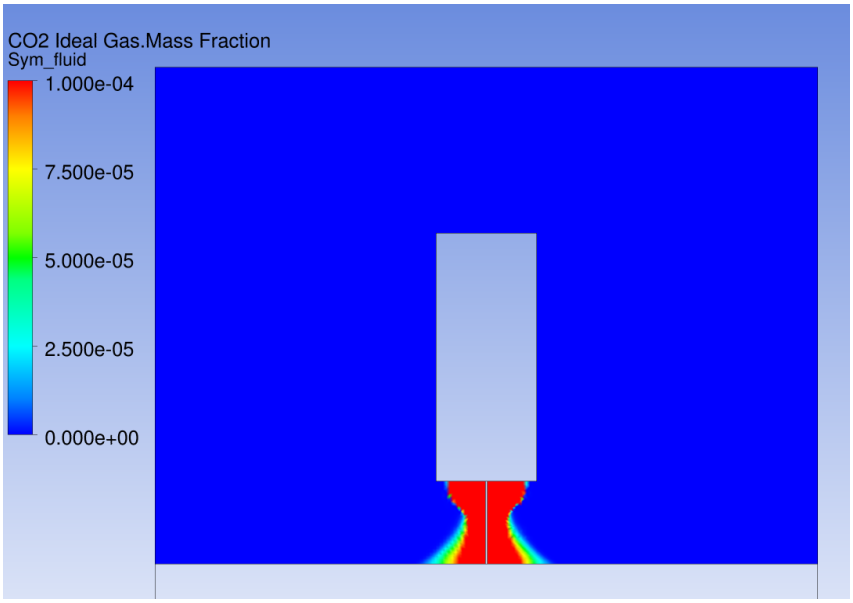

Figure 45, Shield gas mass fraction, design 32

In figures 41-45 it can been seen that the initial expectation of a trade-off between the shield gas and fume suction is well proven. However, the question remains if there are any structures that have acceptable values on both. Figure 46 shows all the results after the MOGA-II optimization on the response surface. Seen here is that there are no designs, within the range used here, that fulfil both the need of shield gas and fume capture. Since the shield gas should almost have a mass fraction of one around the melt (Sandvik, u.d.) the fume capture will not be large. Should for example the minimal need for shield gas be a mass fraction of 95 %, less than 5 % of the fumes would be captured. Notable is that some of the fume released is still in the domain since it is a transient run and would probably be captured later. Regarding the shield gas rate it is also generally high when a high shield gas mass fraction is needed. This means that a larger amount of shield gas is used which goes against the target to minimize shield gas use.

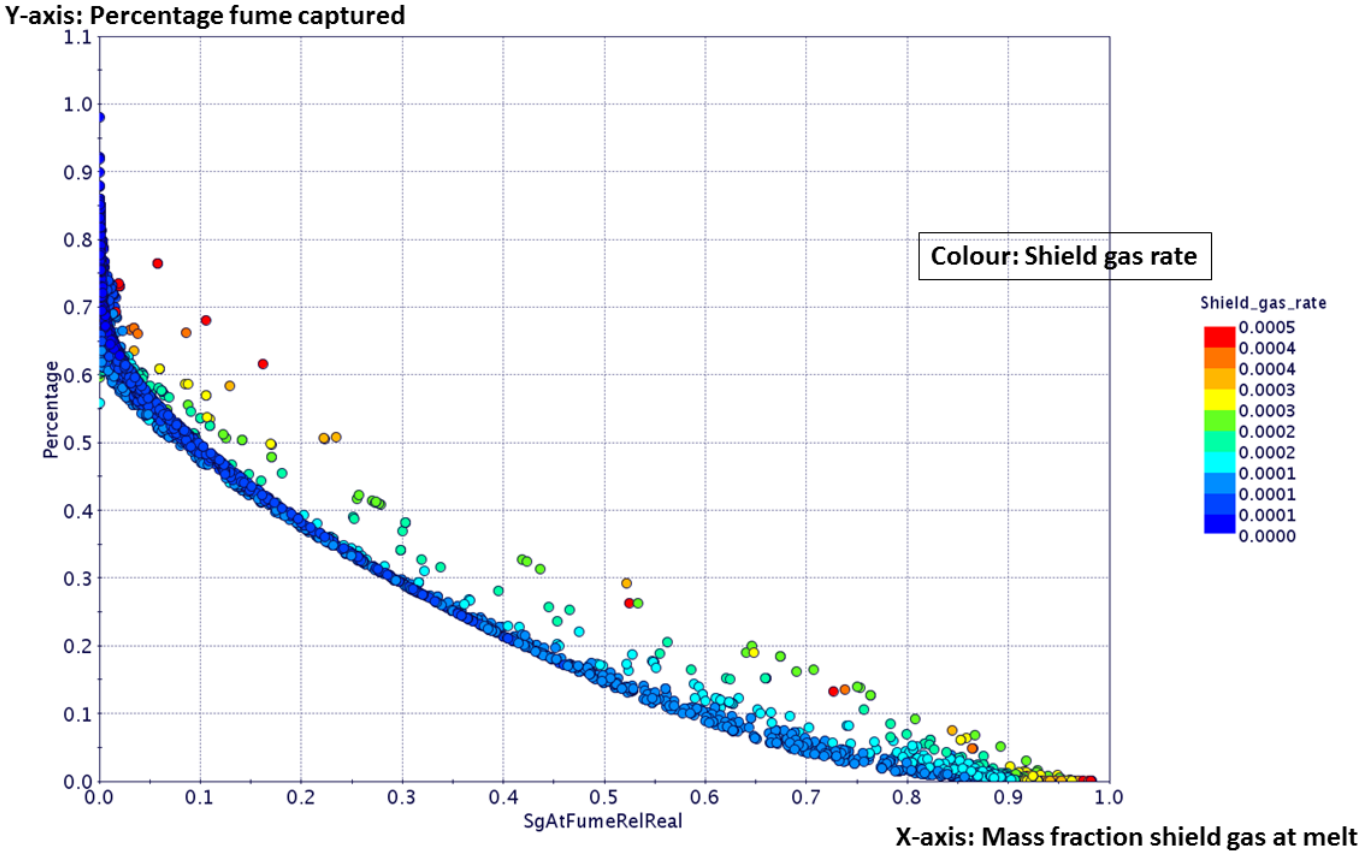

Figure 46, Response surface of percentage of fume captured and mass fraction shield gas at the melt along with the shield gas rate

The final correlations between the different parameters is shown in figure 47. It can be seen that the fume captured is negatively correlated with the shield gas rate and positively correlated with the suction rate. This is an expected behaviour since the shield gas is pushing the fume downwards, making it more difficult to use suction, and a higher suction rate should mean that more fume is captured. Regarding the shield gas mass fraction at the melt, it is reversed correlations in comparison to the fume capture. This means that the trade-off between the two is once again shown. Notable is that the shield gas rate is affecting the results to a greater extent than the suction rate for this specific case and interval.

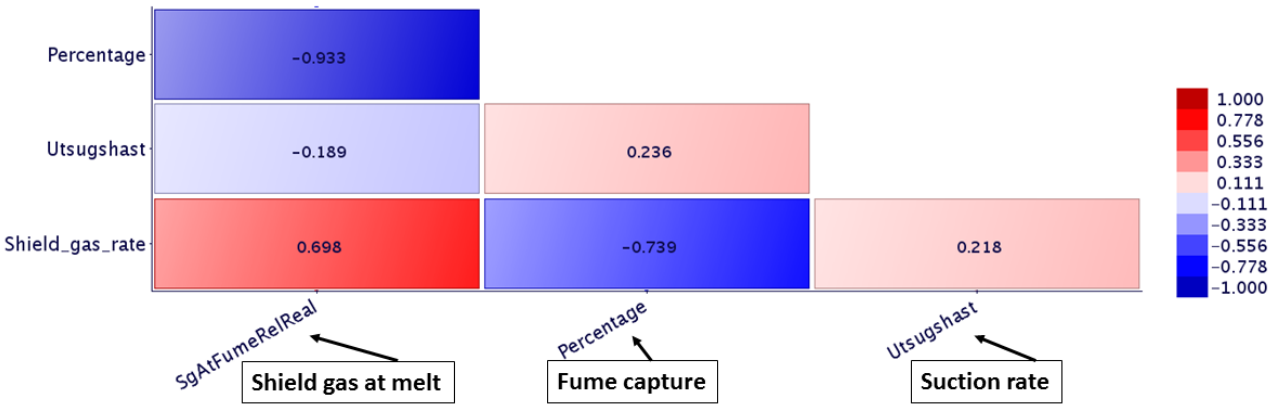

Figure 47, Correlation matrix

8.6. Conclusion and Discussion

Concluded from this optimization is that there are actually no perfect designs. For this specific case it is not possible to obtain a good fume capture as well as sufficient protection of the melt since no design fulfil both of these targets. The shield gas rate also needs to be high, within the interval used here, to obtain good melt protection. This is a problem since the cost for welding rises with this.

Important to know is that more parameters than the two investigated here are expected to affect the results. One example of this is the height at which the on-torch suction is placed. In some cases the fumes are just moving along the handle, due to the vortices created, and it would therefore be possible to place the suction further up the handle and still capture the same amount of fume. A higher placement would also reduce the risk of removing shield gas from the melt protection layer. Another parameter is the size of the shielding gas release area. A smaller area here would mean higher velocity with the same amount of shield gas released. This would then give that the shield gas rate can be lower without losing the needed protection effect. The weld angle is also expected to have an impact on the effectiveness of this. A larger welding angle will probably mean less chance of the fume moving alongside the handle. It will also affect the direction of the shield gas flow and therefore the fume will probably not be pushed downwards in the same manner.

As seen in figure 42 and mentioned in the results section, the vortices created from the shield gas flow will probably catch the fume as well. There are possibilities that this could be practiced to place another suction here since the fume in some sense will be trapped at this position. Another placement of suction could be at the sides of the domain since the shield gas is often pushing the fume in that direction. However, these proposals will have to be investigated further in order to make final conclusions.

One possible source of error is the fact that the fume in some cases is pushed down by the shield gas flow and then slowly reaching upwards. Since the simulations are only run for 0.5 seconds it could be possible that the fume is not reaching the suction area in time. This would then mean that the results are showing less fume capture although the fume at a later point would be fully caught.

Another source of error is that the intervals of input parameters are limited and could possibly give misleading results. More simulations would be needed to be absolutely certain that this is avoided although it is expected that for example a higher suction rate would only mean less shield gas at the melt.

Finally it can be summarized that the geometry used here has no suitable design. However, it is expected that a changed geometry can give results that show a much better performance.

9. Final Conclusion and Discussion

Finally it can be summarized that welding fumes are very much possible to model although a very high temperature is present. One of the problems is that transient simulation is needed in many cases, which means that the simulations are very time consuming. Efforts have in this project been made to reduce the time needed through using a smaller geometry and larger mesh cells in unimportant areas. Still it has not been possible to run any three dimensional simulations for parametric testing and optimization in the scope of this thesis. The two dimensional models can definitely be used to make conclusions and also give a hint of the correlation between certain parameters. However, a fume flow from welding is a three dimensional phenomena and as discussed earlier in this report, the fume tends to flow around the solid parts which is not achieved in two dimensions.

Transient simulations have mostly been used in this project due to the fact that welding fume release has a time dependent behaviour with very high temperatures. Steady state simulations have been tested, but for many cases convergence problems appear and a solution is not possible to obtain. It is also interesting to be able to see what happens during time which is why transient simulations are recommended.

Some convergence problems have occurred in the beginning of some of the transient runs, such as the three dimensional MIG case. The solution to this has been to release the heat over a period of 0.1 seconds instead of all at an instant. Some problems with imbalances in the beginning of the run were also occurring for the three dimensional runs. However this was quite quickly stabilized and therefore accepted.

Parametric testing has shown useful results such as the large effects of high shield gas rate and the smaller effects of high heat release. Regarding the welding angle further testing would be recommended since three dimensional geometry would show a more correct result. However, some conclusions can be made regarding the weld angle such as the fact that it does indeed affect the fume flow much.

The optimization showed that on-torch setup cannot be totally controlled by only using the shield gas rate and suction rate. Although these are important parameters that have a large impact on the flow, more parameters should be tested to obtain an even more reliable result.

10. Future Work

When it comes to future work there are many recommendations from the author's side since twenty weeks is not near enough time to study welding fumes. The proposals listed here covers a wide range of subjects and could easily be split up into a number of different projects.

- Very interesting would be to actually model the fume with the effect of agglomeration. Agglomeration could possibly have a large influence on the particles and is possible to model through mathematical functions that describe the phenomena. This would make it possible to check the size of the particles when they reach the breathing of the welder. The size of the particles is essential for determining the degree of health effects. Smaller particles are generally more dangerous since they reach further into the lungs. A study of particle sizes could then be very useful to reduce this hazard and know where the most dangerous particle are.
- In this project a relatively small domain has been used. In reality, the welding often takes place in larger industry halls. There is also the aspect that the welder's head might be placed further away from the weld than the domain used here. It would therefore of course be interesting to study a larger area. Recommendations of reducing the computational time needed have already been briefly discussed but include using boundary conditions from a smaller domain which would mean that it is not needed to calculate all the cells in the larger domain for the entire simulation.
- Other recommendations would be to run the parametrization and optimization in three dimensions instead of in two. The problem with two dimensions is that no flow is allowed to pass the handle or electrode. As have been seen in this project, the flow sometimes makes this move and therefore the two dimensions are not entirely sufficient. This would of course be very time consuming but yet very interesting and all preparations have already been made in this project. It would also be exciting to see when it is sufficient to run in two dimensions and when it is not.
- In the parametrization and optimization it would possibly be interesting to evaluate a wider range of values on the parameters as well. More values gives a better foundation for making relevant conclusions. It is also possible that some important values that would show beneficial designs have been missed in this project. More different parameters could also give effects.
- The fact that the material of the electrode and workpiece affect the welding fumes is known. However, the size of the effect has only been briefly tested in this project. There are apart from thermal conductivity in the materials also affects from the fume composition and fume rate. Here it has been assumed that the fume movement would not be considerably affected from this but it could still be interesting. For example it could be combined with the agglomeration model where the change of material could possibly have much greater effects than in this project.
- Another interesting geometry feature to evaluate would be to use a finite workpiece. It has been seen that vortices are present in the fume flow and it could therefore be possible that the fume gets "stuck" beneath the workpiece should it not be infinite as in this project. Other geometries that are actually used in welding such as welding in a corner would also be of value to investigate.
- Since a real welding environment actually contains a welder it would be possible to also include this in the geometry of the model. For example the welders arm could be modelled. To model the ventilation in the room or simulate a door opening could also affect the fume movement and so be interesting to investigate. Even outdoor welding could be an exciting subject since there are a lot of factors that do not occur indoors. A model for outdoor welding would probably need many assumptions and would also have to be simplified in order to give results in a relevant time frame.

11. References

A.Lovison, E., 2010. *Adaptive sampling with a Lipschitz criterion for accurate metamodelling,* s.l.: Enginsoft.

ANSYS CFX, n.d. *ANSYS CFX Help,* s.l.: s.n.

ANSYS Fluent, n.d. *ANSYS FLUENT Help,* s.l.: ANSYS.

Astronomy Group, University of St Andrews, n.d. [Online]
Available at: http://www-star.st-and.ac.uk/~kw25/teaching/mcrt/mcrt_l01_2015.pdf
[Accessed 23 03 2016].

B.Sundén, 2006. *Värmeöverföring.* Lund: Studentlitteratur.

Engineering toolbox, n.d. [Online]
Available at: http://www.engineeringtoolbox.com/
[Accessed 03 02 First use: 2016].

EPA, n.d. *Healt Effects of Ozone in the General Population.* [Online]
Available at: https://www3.epa.gov/apti/ozonehealth/population.html
[Accessed 12 06 2016].

ESAB, n.d. [Online]
Available at:
http://www.esab.se/se/se/products/index.cfm?fuseaction=home.product&productCode=410005&tab=2
[Accessed 22 04 2016].

Fluent incorporated, n.d. [Online]
Available at: http://jullio.pe.kr/fluent6.1/help/html/ug/node483.htm
[Accessed 23 04 2016].

Foremen Training Institute Bangalore, n.d. *STTI worker union.* [Online]
Available at: http://sttiworkerunion.weebly.com/uploads/1/0/6/9/10694229/mig-srao_apex_prg.doc
[Accessed 08 03 2016].

J.Tu, G. C., 2013. *Computational Fluid Dynamics - A Practical Approach.* Oxford, GB: Butterworth-Heinemann.

K.Malmqvist, G. M. R., 1980. *Luftföroreningar vid svetsning - Karakterisering av svetsrök,* Lund: Institutionen för kärnfysik, Lunds universitet.

M.Pavlovich Bulat, P. B., 2013. Comparison of Turbulence Models in the Calculation of Supersonic Separated Flows. *World Applied Sciences Journal 27,* pp. 1263-1266.

M.Sommerfeld, B. W. R., 2008. *Best Practice Guidelines for Computational Fluid Dynamics of Dispersed Multiphase Flows,* s.l.: European Research Community On Flow, Turbulence And Combustion.

Merck Millipore, n.d. *Millipore Filter Specifications.* s.l.:s.n.

MIG-welding, n.d. [Online]
Available at: http://www.mig-welding.co.uk/tig-setup.htm
[Accessed 16 04 2016].

Netwelding, n.d. [Online]
Available at: http://www.netwelding.com/MIG_Flow%20Rate-Chart.htm
[Accessed 24 02 2016].

OSHA, n.d. *Health Effects of Hexavalent Chromium.* [Online]
Available at: https://www.osha.gov/OshDoc/data_General_Facts/hexavalent_chromium.pdf
[Accessed 02 06 2016].

OSHA, n.d. *OSHA Fact Sheet.* [Online]
Available at: https://www.osha.gov/OshDoc/data_General_Facts/carbonmonoxide-factsheet.pdf
[Accessed 12 06 2016].

R.F.Heile, D., 1975. Particulate Fume Generation in Arc Welding Processes.

S.Poles, 2003. *MOGAII - An Imporved Multi-Objective Genetic Algorithm,* s.l.: Esteco.

Sandvik, n.d. *Shielding the weld.* [Online]
Available at: http://smt.sandvik.com/en/products/welding-products/shielding-gases/
[Accessed 30 05 2016].

V.Mali, S., n.d. *Learncax.* [Online]
Available at: https://www.learncax.com/knowledge-base/blog/by-category/cfd/basics-of-y-plus-boundary-layer-and-wall-function-in-turbulent-flows
[Accessed 18 05 2016].

Wolfram Mathworld, n.d. *Quadratic Surface.* [Online]
Available at: http://mathworld.wolfram.com/QuadraticSurface.html
[Accessed 01 06 2016].

12. Appendix

12.1. On-torch Optimization

Table 10, DOE, first 24 designs for on-torch suction, unscaled values

Design ID	Suction rate [m/s]	Shield gas rate[kg/s]
0	9.25759	1.24E-02
1	8.69869	9.99E-03
2	2.82448	3.96E-03
3	6.46777	1.63E-02
4	6.96817	1.77E-03
5	1.21915	8.59E-03
6	5.49433	7.10E-03
7	3.78649	1.77E-02
8	2.82592	1.59E-02
9	1.24588	1.48E-02
10	2.87623	1.48E-02
11	1.91629	3.93E-05
12	7.53733	6.23E-03
13	1.96498	1.86E-02
14	1.71577	5.78E-03
15	1.99513	7.88E-04
16	1.06624	5.91E-03
17	5.63194	1.03E-03
18	1.96705	9.79E-03
19	3.94804	3.93E-05
20	2.86021	3.93E-05
21	1	5.32E-03
22	3.94543	5.89E-03
23	4.53493	3.93E-05

Table 11, Design values from incremental space filler method, unscaled values

Design ID	Suction rate [m/s]	Shield gas rate [kg/s]
24	1.6282	0.00004
25	6.1283	0.00983
26	6.1283	0.00004
27	1.6326	0.00983
28	3.8783	0.00493
29	8.3826	0.01472
30	3.8783	0.01473
31	8.3783	0.00494
32	8.3848	0.00983

Table 12, Design values from Lipschitz sampling method, unscaled values

Design ID	Suction rate [m/s]	Shield gas rate [kg/s]
33	3.1232	8.24E-03
34	3.5919	2.28E-03
35	7.2561	8.81E-03
36	5.9831	4.11E-03
37	4.0892	1.03E-02